

Implications of Analyticity to Solution of Schwinger-Dyson Equations in Minkowski Space

Vladimír Šauli

Dep. of Theor. Phys. NPI Řež near Prague, CAS, CZ

Abstract. We review some recent developments in nonperturbative studies of quantum field theory (QFT) using the Schwinger-Dyson equations formulated directly in Minkowski space. We begin with the introduction of essential ideas of the integral representation in QFT and a discussion of renormalization in this approach. The technique based on the integral representation of Green's functions is exploited to solve Schwinger-Dyson equations in several quantum field models, eg. in scalar models and in strong coupling QED_{3+1} in the quenched and in the unquenched approximation. The phenomenon of dynamical chiral symmetry breaking in regularized theory is touched. In QCD, the analyticity of gluon propagator on the complex momentum square plane is exploited to continue some recent lattice data to timelike momentum axis. We find non-positive absorptive part contribution in the Landau gauge gluon propagator which is in agreement with some other new recent analyzes.

1 Introduction

This work is devoted to studies of quantum field models with strong coupling. The *Schwinger-Dyson equations* (SDEs) in momentum representation are solved and analyzed in Minkowski space. In this introduction our motivations, broad contexts and main results are briefly summarized.

These days the experimentally accessible particle physics is being described in the framework of the (effective) quantum field theory (QFT) by the Standard model of the strong and electroweak interactions with the gauge group $SU_c(3) \otimes SU_L(2) \otimes U_Y(1)$. When the perturbation theory is applicable the observables follow from the Lagrangian in relatively straightforward way: the corresponding S-matrix elements are generated from n-point *Green's functions* (GFs) which are calculated and regularized/renormalized order by order according to the standard rules. Order by order perturbation theory can be naturally generated from expansion of SDEs: an infinite tower of coupled equations connecting

successively higher and higher points GFs. The GFs themselves are not observable and they contain some redundant information: off-shell behavior (connected e.g. with a possible field redefinition) and also some other remnants of the particular calculation scheme employed, e.g., gauge fixing parameters and renormalization scales. If the program of the perturbation theory is carried out consistently up to the certain order, the observables should be independent of all these unphysical parameters.

Needless to say, many phenomena exist outside the reach of the perturbation theory approach, especially when the strong sector of the Standard model – *Quantum Chromodynamics* (QCD) – or some extensions of the Standard model are concerned: bound states, confinement, dynamical mass generation etc. Going beyond perturbation theory requires development of elaborated approaches and sophisticated tools, especially in the strong coupling regime. Number of such approaches has been pursued: lattice theories, Feynman-Schwinger representation, nonperturbative treatment of SDEs, bag models These days neither of them provides such a clear and unambiguous understanding of the physics as we are accustomed to in the perturbative regime. The lattice approach clearly stands by its own, since it does not rely on any uncontrollable approximations: just the brute force discretization of path integrals is employed. Lattice “data” should (in principle) provide as good representation of the studied dynamics as real ones (with additional merit of allowing to vary the dynamical input), but converged unquenched results are in most cases just not available as yet (however for some recent progress in QCD see [1],[2],[3]).

In this work we deal with the nonperturbative solutions of the SDEs. If one could solve the full infinite set of SDEs, the complete solution of the QFT will be available, coinciding with the results of converged lattice calculations. In reality one has to truncate this set of equations: the main weakness of SDEs phenomenology is the necessity to employ some Ansatz for higher Greens functions. The reliability of these approximations can be estimated by comparison with the known perturbation theory result in the regime of a soft coupling constant and by comparison with the lattice data (and/or results of alternative approaches like $\bar{\Phi}$ -derivable effective action, etc.) where available. The recent results (see e.g. reviews [4, 5, 6, 7] and references therein) provide some encouragement: they suggest that SDEs are viable tool for obtaining (eventually) the truly nonperturbative answers for plethora of fundamental questions: *dynamical chiral symmetry breaking*, *confinement* of colored objects in QCD, the high temperature superconductivity in condensed matter (modeled [8] by QED_{2+1}). In the QCD sector there is also a decent agreement with some experimental data: for meson decay constants like F_π , evolution of quark masses to their phenomenologically known (constituent) values, bound states properties obtained from Bethe-Salpeter or Fadeev equations (the part of SDEs).

The recent solutions of SDEs [7],[9] nicely agree with the lattice data [2, 10, 11] (the explicit comparison is made in [9, 7, 12]). Thus, encouraging connections between results of SDEs studies and fundamental theory (QCD) and/or various phenomenological approaches (chiral perturbation theory, constituent quark model, vector meson dominance . . .) are emerging.

Most of these results were obtained by solution of SDEs in Euclidean space. One of the main goal of this work is to develop an alternative approach allowing to solve them directly in Minkowski space. In this method (generalized) *spectral decompositions* of the GFs are employed, based on their analytical properties. The main merit of this approach is possibility to get solutions both for spacelike and timelike momenta. Techniques of solving SDEs directly in Minkowski space are much less developed than the corresponding Euclidean ones. Therefore most of this paper deals with developing and testing such solutions on some simple QFT models.

For large class of nonasymptotically free theories running couplings – calculated from perturbation theory – diverge at some finite but usually large spacelike scale. If perturbation theory results are taken literally, stretching them clearly beyond the range of applicability, also the QCD coupling develops singularity for low momenta squared. In the latter case the lattice as well as SDEs results suggest that nonperturbative effects alter behavior of running coupling $\alpha_{QCD}(q^2)$ significantly, situation for nonasymptotically free is less clear. This is why we pay special attention to behavior of our solutions in the region of high momenta.

The paper is organized as follows. Section 2 serves as an introduction: some well known general results and useful textbooks formulas are collected and basics of the formalism employed later are discussed. The integral representation for GFs are reviewed and the calculation of dispersion relation is exhibited at one and two loop example. Section 3 is devoted to the simple scalar model $a\Phi^3 + b\Phi^4$ for pedagogical reason. The momentum space SDE is converted to the Unitary Equation for propagator spectral density. The Unitary Equation is shown to be real equation where the singularity accompanying usual Minkowski space calculation are avoided. The relativistic problem of bounds states as an intrinsically nonperturbative phenomena is briefly reviewed in this Section too.

Section 4 represents study of the SDEs in 3+1 QED. For this purpose we improve and reorganize the Unitary Equations already particularly found in the papers [13, 14] in a way that the numerical obstacles with singular integral kernels are avoided. Due to this the resulting numerical solutions of our Unitary Equations become more stable and accurate.

One should mention at this point a possibility of getting the solutions of the SDEs in Minkowski space with the help of analytical continuation of the Euclidean ones. Nevertheless in simple cases it can be successful: we have recently done this for the gluon form factor and we present our results in the Section devoted to the QCD.

Section 5 offers some further comments on spectral treatment of Schwinger-Dyson equations and possible further progress is discussed.

Section 6 presents the known attempt to solve the SDEs in QCD in Minkowski space. Furthermore, $SU(3)$ Yang-Mills, i.e the pure gluodynamics is discussed there and analytical behavior of gluon propagator is deduced by the analytical continuation from Euclidean space to the analyticity domain boundary. To obtain numerically stable analytical continuation is not an easy task and attempts to perform it are rare. As an input data we have used recently obtained lattice data [1].

2 Integral Representations in Quantum Field Theory

Solutions of the SDEs in this work are based on integral representations of Green's functions. In this Section we briefly review their derivation and then present two illustrative examples from the Φ^4 model.

The development of spectral techniques can be stimulated by following consideration. Let us assume that any GF can be written as an expansion of skeleton contributions, i.e., the diagrams where the propagators corresponding to the internal lines are exact. If we further assume the analyticity of these propagators (in the sense discussed in the next text), then one can apply the whole well established knowledge about the analytical structure of Feynman diagrams. The singularity structure of each Feynman graph allows a simple connection between momentum dependence in spacelike and timelike regime, i.e., between Euclidean and Minkowski space. That the equations of motions which hold between Green's functions, i.e. SDEs , can be translated into the corresponding relations between spectral functions was already known half century ago [15, 16]. The renormalization program has been carried in the terms of spectral function as well.

This was also the basis of historical development of the dispersion relation (for summary see [17]) and of the Mandelstam representation in the late 50's [18]. Many of these efforts have been summarized in the standard textbook of that time, see e.g. [19]. This book represents deductive approach to S-matrix theory, the subject rather popular in particle physics at that time. Fortunately, being mainly based on the analysis of Feynman graphs (and their infinite sum), the methods reviewed in this book (including also asymptotic high energy behavior, Regge poles,...) survive and have found their appropriate use, even after the time when QCD was born and the trust to quantum field theory was renewed.

2.1 The Källén–Lehmann Representation

In this Section we remind the derivation of the Umezawa–Kamefuchi–Källén–Lehmann *spectral representation* (SR) [20, 21, 22, 23] for a two-point Green's function.

Let us consider the vacuum expectation value of the product of two real scalar fields $\langle 0|\phi(x)\phi(y)|0 \rangle$. To arrive at the desired expression for the propagator

$$iG(x - y) = \langle 0|T\phi(x)\phi(y)|0 \rangle \quad (1)$$

one inserts the identity operator

$$\hat{1} = |0 \rangle \langle 0| + \sum_{\lambda} \int \frac{d^3\mathbf{p}}{(2\pi)^3 2\sqrt{\mathbf{p}^2 + m^2}} |\lambda_{\mathbf{p}} \rangle \langle \lambda_{\mathbf{p}}|, \quad (2)$$

between the fields $\phi(x)$ and $\phi(y)$ in (2.1):

$$\langle 0|\phi(x)\phi(y)|0 \rangle = \sum_{\lambda} \int \frac{d^3p}{(2\pi)^3 2\sqrt{p^2 + m^2}} \langle 0|\phi(x)|\lambda_{\mathbf{p}} \rangle \langle \lambda_{\mathbf{p}}|\phi(y)|0 \rangle \quad (3)$$

where the sum runs over complete set of λ -particles states $|\lambda_{\mathbf{p}} \rangle$ with given momentum \mathbf{p} . It is assumed that a spontaneous symmetry breaking does not take

place, i.e., that $\langle 0|\phi(x)|0 \rangle = 0$; if it does a space-time independent constant appears on the r.h.s. Making use of the translational invariance, transformation properties in respect to the Lorentz boost:

$$\begin{aligned} \langle 0|\phi(x)|\lambda_{\mathbf{p}} \rangle &= \langle 0|e^{i\hat{P}\cdot x}\phi(0)e^{-i\hat{P}\cdot x}|\lambda_{\mathbf{p}} \rangle \\ &= \langle 0|\phi(0)|\lambda_{\mathbf{p}} \rangle e^{-i p \cdot x}|_{p_0=E_p} = \langle 0|\phi(0)|\lambda_0 \rangle e^{-i p \cdot x}|_{p_0=E_p} \end{aligned} \quad (4)$$

and of the integral representation of the step function, one gets for $x_0 > y_0$

$$\langle 0|\phi(x)\phi(y)|0 \rangle_{x_0 > y_0} = i \sum_{\lambda} \int \frac{d^4 p}{(2\pi)^4} \frac{\exp(-i p \cdot (x - y))}{p^2 - m_{\lambda}^2 + i\epsilon} |\langle 0|\phi(0)|\lambda_0 \rangle|^2. \quad (5)$$

Taking (5) together with an analogous expression for an opposite time ordering gives the Feynman propagator in the form

$$G(x - y) = \int d\omega \bar{\sigma}(\omega) D(x - y, \omega), \quad (6)$$

$$\bar{\sigma}(\omega) = \sum_{\lambda} \delta(\omega - m_{\lambda}^2) |\langle 0|\phi(0)|\lambda_0 \rangle|^2, \quad (7)$$

$$G(p) = \int d\omega \frac{\bar{\sigma}(\omega)}{p^2 - \omega + i\epsilon}, \quad (8)$$

where $\bar{\sigma}(\omega)$ is a positive spectral density (*the Lehmann function*) and D stands for free-particle propagator with 'mass' $\sqrt{\omega}$, i.e.

$$D(x - y, \omega) = \int \frac{d^4 p}{(2\pi)^4} \frac{\exp(-i p \cdot (x - y))}{p^2 - \omega + i\epsilon} \quad (9)$$

and $D(p, \omega)$ is its Fourier transform.

To sum it up: the derivation of the spectral representation of the two-point Green's function is based on three assumptions:

- the Poincare invariance of the theory,
- existence of the physical states $|\lambda_{\mathbf{p}} \rangle$,
- the completeness relation (2).

The physical propagator usually contains the single particle pole and the continuous part stemming from the interaction. Therefore we typically get:

$$G(p) = \int d\omega \bar{\sigma}(\omega) D(p, \omega) = r D(p, m^2) + \int d\omega \sigma(\omega) D(p, \omega), \quad (10)$$

where $D(p, m^2)$ is a free propagator with the physical mass, r is a residuum at $p^2 = m^2$, and σ is a nonsingular continuous part, nonzero above certain kinematical threshold. For the free scalar field $r = 1$ and $\sigma = 0$.

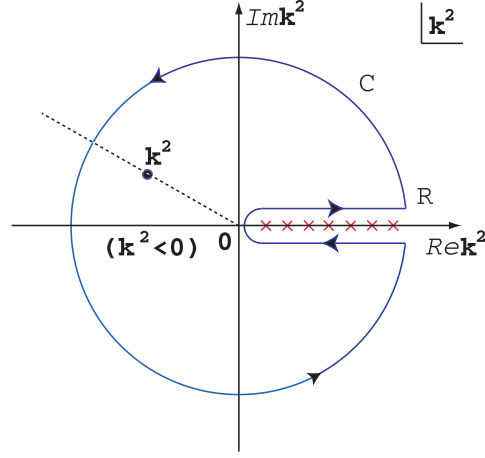


Figure 1. The position of singularities on the complex momentum plane with the sketched integration contour C used in the main text. The singularities can appear only for $Re k^2 > 0$ (crosses).

2.2 Analyticity

Suppose that the complex function $f(z)$ is analytical in the whole complex plane of $z \equiv k^2$ except for the positive real axis $z > 0$. Then we can choose a closed loop C in the complex k^2 plane as in Fig. 1, such that the complex function $f(z)$ is analytical inside and on the loop C . For a reference point k^2 inside C , the Cauchy integral formula tells us that

$$f(k^2) = \frac{1}{2\pi i} \oint_C dz \frac{f(z)}{z - k^2} \quad (11)$$

$$= \frac{1}{2\pi i} \int_0^R dz \frac{f(z + i\epsilon) - f(z - i\epsilon)}{z - k^2} + \frac{1}{2\pi i} \oint_{|z|=R} dz \frac{f(z)}{z - k^2}, \quad (12)$$

where we have separated the integral into two pieces: one is the contribution from the paths above and below the positive real axis; the other is the contribution to the integral over the circle of radius R .

First, making use of the fact that $f(k^2)$ is real for $k^2 < s_{min}$ for some nonnegative s_{min} (by assumption, at least for $k^2 < 0$, i.e., for spacelike k), it follows from the Schwartz reflection principle that for $Re z > s_{min}$ it holds $f(z - i\epsilon) = f^*(z + i\epsilon)$ and hence $f(z + i\epsilon) - f(z - i\epsilon) = f(z + i\epsilon) - f^*(z + i\epsilon) = 2i \text{Im} f(z + i\epsilon)$. Hence the first term in r.h.s. of (12) picks up the discontinuity (the imaginary part) of the function $f(z)$ along the positive real axis.

Next, the circle $|z| = R$ is parameterized as $z = Re^{i\theta}$:

$$f(k^2) = \frac{1}{\pi} \int_0^R dz \frac{\text{Im} f(z + i\epsilon)}{z - k^2} + \int_0^{2\pi} \frac{d\theta}{2\pi} \frac{Re^{i\theta} f(Re^{i\theta})}{Re^{i\theta} - k^2}. \quad (13)$$

The second term on the r.h.s. of this equation has the bound

$$\left| \int_0^{2\pi} \frac{d\theta}{2\pi} \frac{Re^{i\theta} f(Re^{i\theta})}{Re^{i\theta} - k^2} \right| \leq \int_0^{2\pi} \frac{d\theta}{2\pi} \frac{R|f(Re^{i\theta})|}{|Re^{i\theta} - k^2|} \leq \max_{0 < \theta < 2\pi} |f(Re^{i\theta})| \frac{R}{R - |k^2|}. \quad (14)$$

Now we wish to take the radius R of the circle to infinity. Thus, if $|f(z)| \rightarrow 0$ as $|z| \rightarrow \infty$, then the second term has no contribution as $R \rightarrow \infty$ and we arrive at the desired Dispersion Relation (DR):

$$f(k^2) = \frac{1}{\pi} \int_0^\infty dz \frac{\text{Im} f(z)}{z - k^2 + i\epsilon}. \quad (15)$$

This can also be written as

$$f(k^2) = \int_0^\infty ds \frac{\rho(s)}{s - k^2 + i\epsilon}, \quad \rho(s) := \frac{1}{\pi} \text{Im} f(s), \quad (16)$$

then the SR for propagator (10) exactly coincides with the DR (16).

To solve the SDEs in Minkowski space we will need also integral representation for the inverse of propagator. In the renormalizable theories such spectral functions often do not vanish at infinity. This can be already viewed from the identity

$$\text{Im} f(z)^{-1} = -|f(z)|^{-1} \text{Im} f(z), \quad (17)$$

where we identified the function f with the propagator function G . Then one makes the momentum space subtraction(s) and arrives at modified dispersion relations. For instance, let us define a new function

$$f_R(\zeta; z) = f(z) - f(\zeta), \quad (18)$$

and assume that $f_R(z) \rightarrow 0$. This gives the once-subtracted DR:

$$f_R(\zeta; z) = \frac{(k^2 - \zeta)}{\pi} \int_0^\infty dz \frac{\text{Im} f(z)}{(z - k^2 + i\epsilon)(z - \zeta)}. \quad (19)$$

If the other divergence occurs, one can go on and subtract the next term in the Taylor expansion of $f(z)$.

2.3 Dispersion relations in scalar theory

In this Section we derive the DRs first for the one-loop elastic two particle scattering amplitude in the scalar Φ^4 theory without spontaneous symmetry breaking, i.e., in the QFT given by Lagrangian:

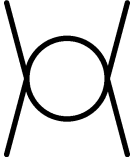
$$\begin{aligned} \mathcal{L} &= \frac{1}{2} \partial_\mu \Phi \partial^\mu \Phi - \mathcal{V}(\Phi), \\ \mathcal{V}(\Phi) &= \frac{m_0^2}{2} \Phi^2 + g_0 \Phi^4, \end{aligned} \quad (20)$$

where the global minimum condition $V(\Phi = 0) = 0$ entails the zero value of the field vacuum expectation value.

Next, as a less trivial example, we offer a detailed original proof of DR for a two-loop self-energy function in the (off-shell) momentum subtraction renormalization scheme. The calculation is performed for the noninteger dimension $D = 4 - \epsilon$, the limit $\epsilon \rightarrow 0$ is taken after the appropriate subtractions. However the results on imaginary part of the sunset diagram was already obtained several years ago by the Cutkosky rules approach [24] (see also [25] for general case in n-dimensions) the derivation presented here follows an ideas of renormalization realized directly in momentum space.

2.4 Scattering amplitude at one skeleton loop

The scattering matrix in Φ^4 theory is composed from the four-point Green's function. The one-loop skeleton contribution to the irreducible GF reads

$$\Gamma_0^{(4)}(l^2) = \text{Diagram} = -i \frac{(4!g_0)^2}{2} \int \frac{d^d k}{(2\pi)^d} G(k+l)G(k), \quad (21)$$


where g_0 is a bare coupling and G represents fully dressed propagator (10). Substituting the Lehmann representation for G gives

$$\begin{aligned} \Gamma_0^{(4)}(l^2) &= \frac{(4!g_0)^2}{2} \int d\alpha_1 \bar{\sigma}(\alpha_1) \int d\alpha_2 \bar{\sigma}(\alpha_2) I_0(l^2), \\ I_0(l^2) &= \int \frac{d^d k}{(2\pi)^d} D(k+l, \alpha_1) D(k, \alpha_2). \end{aligned} \quad (22)$$

Thus, the derivation of DR reduces to the familiar ‘‘perturbative’’ spectral representation of the scalar integral $I_0(l^2)$. The unrenormalized vertex Γ_0 requires just one subtraction due to the presence of logarithmic UV divergence

$$\begin{aligned} \Gamma^{(4)}(l^2, \zeta_g) &= \Gamma_0^{(4)}(l^2) - \Gamma_0^{(4)}(\zeta_g), \\ \Gamma^{(4)}(l^2, \zeta_g) &= \frac{(4!g(\zeta_g))^2}{2} \int d\alpha_1 \bar{\sigma}(\alpha_1) \int d\alpha_2 \bar{\sigma}(\alpha_2) I_R(l^2), \\ I_R(l^2) &= \int_{(\sqrt{\alpha_1} + \sqrt{\alpha_2})^2}^{\infty} d\omega \frac{(l^2 - \zeta_g) X(\alpha_1, \alpha_2, \omega)}{(\omega - \zeta_g)(l^2 - \omega + i\epsilon)}, \end{aligned} \quad (23)$$

where the function X is defined as

$$\begin{aligned} X(a, b; \omega) &= \frac{\lambda^{1/2}(a, b, \omega)}{\omega} \Theta(\omega - (\sqrt{a} + \sqrt{b})^2), \\ \lambda(x, y, z) &= x^2 + y^2 + z^2 - 2xy - 2yz - 2xz. \end{aligned} \quad (24)$$

and ζ_g is the (square of) renormalization scale. In order to define the renormalized coupling $g(\zeta_g)$ we choose the function $\Gamma^{(4)}(l^2, \zeta_g)$ to be renormalized loop contribution of quartic vertex and include the infinite constant $\Gamma_0(\zeta_g^2)$ into the counter-term part of g_0 . The full scattering amplitude $M(s, t, u)$ in the considered

approximation is the sum of the infinite chain of the irreducible contributions defined above:

$$M(s, t, u) = 4!g(\zeta_g) + \sum_{x=s,t,u} \frac{\Gamma^{(4)}(x, \zeta_g)}{1 - \Gamma^{(4)}(x, \zeta_g)}, \quad (25)$$

where one common renormalization scale ζ_g was used to renormalize GF. Γ in each channel characterized by the Mandelstam variable s, t, u (labeling incoming (outgoing) momenta $p_{1,2}$ ($p_{3,4}$), they are $s = (p_1 + p_2)^2, t = (p_1 - p_3)^2, u = (p_1 - p_4)^2$). The first term on the l.h.s. of Eq. (25) represents the tree value of the amplitudes M .

Several important remarks can be made about the obtained result.

- Integrating the single particle contribution we explicitly see that the vertex becomes complex for the timelike $x > 4m^2$ and its absorptive part reads:

$$\begin{aligned} \text{Im } \Gamma(t^2) &= \frac{g^2(\zeta_g)}{16\pi} \left[r^2 \sqrt{1 - \frac{4m^2}{\omega}} \Theta(\omega - 4m^2) + 2r \int_{9m^2}^{\infty} d\alpha \sigma(\alpha) X(\alpha, m^2, \omega) \right. \\ &\quad \left. + \int_{9m^2}^{\infty} d\alpha_2 \sigma(\alpha_2) \int_{9m^2}^{\infty} d\alpha_1 \sigma(\alpha_1) X(\alpha_1, \alpha_2, \omega) \right], \end{aligned} \quad (26)$$

which is explicitly independent on the renormalization scale ζ_g .

- perturbation theory is trivially reproduced. Assuming $r \simeq 1$ the one-loop result in the perturbation theory is given by the first term in (26).
- The absorptive part does not vanish for large momenta, it is a constant. For fixed momentum the naive limit $\zeta_g \rightarrow \infty$ cannot be performed. Taking this explicitly then the original log. divergence reappear again. It is impossible to define infinite momentum frame renormalization scheme (the so called Weinberg scheme [26]).
- The summation of the irreducible contributions leads to the Landau ghosts in the amplitudes and the renormalized coupling can not be reasonably defined without some regulators. This pathology is manifest already at the one-loop level. This is because the Φ^4 theory is the (probably the best known) example of the nonasymptotically free theory.

2.5 DR for sunset diagram in momentum subtraction renormalization scheme

In the relation (26) knowledge of the Lehmann function σ is required. It can be taken from the perturbation theory or some improved approximation of the full result can be used. To this end we continue with derivation of a similar relation for the two-point Green function. The renormalized inverse propagator is given by

$$G^{-1}(p^2) = p^2 - m^2(\zeta) - \Pi_R(\zeta; p^2), \quad (27)$$

where Π_R is the renormalized two-point proper self-energy function:

$$\Pi_R(\zeta; p^2) = \Pi(p^2) - \Pi(\zeta) - \left. \frac{d\Pi(p^2)}{dp^2} \right|_{p^2=\zeta} (p^2 - \zeta). \quad (28)$$

In massive ϕ^4 the spectral function is nonzero when $p^2 > 9m^2$, otherwise it is zero.

2.6 Perturbation Theory Integral Representation in renormalizable theories

The Perturbation Theory Integral Representation (PTIR) [27] is a natural extension of the Lehmann representation for the propagator to n -point Green's functions. The PTIR allows to express the amplitudes as integrals over weight functions and a momenta-dependent denominator with known singularity structure. Since the Feynman parametric integral always exists for any Feynman diagram defined by the perturbation theory, one can always define an integral representation such that the number of independent integration parameters is equal to that of invariant squares of external momenta. The general expression for n -point amplitudes, which is considered to be a sum of all Feynman diagrams with n external legs, has been derived by Nakanishi [27] for scalar theories with nonderivative couplings. The PTIR is unique for unrenormalized amplitudes. The general proof of the Uniqueness Theorem can be also found in the Nakanishi's book [27]. The renormalized 2,3,4-point vertices can differ only by the presence of subtraction polynomials as follows from renormalization procedure. The coefficients of the subtraction polynomials then depend on the renormalization scheme employed.

For theories with interactions containing field derivatives or theories with particles of nonzero spin similar results to all order of perturbation theory have never been proved, since tensor and spinor structure of corresponding expressions becomes rather complicated with increasing number of external legs of Feynman diagrams. We do not feel too discouraged by this: the (generalized) PTIR can always be deduced for a given Feynman diagram. Indeed, if we assume the analyticity of the lowest point Green's function -the propagators- then it is sure that the PTIR is derivable for skeleton diagram under consideration.

In what follows we briefly review examples of PTIR for scalar amplitudes. We start with PTIR for the two-point correlation function $\Pi(p^2)$, already discussed in detail above. Recall that the expression for unrenormalized self-energy reads

$$\Pi_0(p^2) = \int dx \frac{\rho(x)}{p^2 - x + i\epsilon}. \quad (34)$$

The renormalized $\Pi_R(p^2)$ turns out to be

$$\Pi_R(p^2) = a + bp^2 + \int dx \frac{\rho(x)(p^2 - \zeta)^2}{(p^2 - x + i\epsilon)(x - \zeta)^2}, \quad (35)$$

where the finite coefficients a, b are characteristic of a given but arbitrary renormalization scheme. Their size indicates how a given scheme employed differs from the momentum subtraction renormalization scheme where $a, b = 0$, since the coefficients

$$\int dx \frac{\rho(x)}{\zeta - x + i\epsilon} \quad ; \quad \frac{d}{dp^2} \left[\int dx \frac{\rho(x)}{p^2 - x + i\epsilon} \right] \Big|_{p^2=\zeta} \quad (36)$$

are fully absorbed into the Lagrangian counter-terms in this scheme.

For the three-leg vertex function $\Gamma(p_1, p_2)$ analysis of contributing Feynman diagrams leads to the PTIR derived by Nakanishi:

$$\Gamma(p_1, p_2) = \int_0^\infty d\alpha \prod_{i=1}^3 \int_0^1 dz_i \delta(1 - \sum_{i=1}^3 z_i) \frac{\rho_3(\alpha, \mathbf{z})}{\alpha - (z_1 p_1^2 + z_2 p_2^2 + z_3 p_3^2) - i\epsilon}, \quad (37)$$

where the momenta are conserved $p_1 + p_2 + p_3 = 0$, the invariant squares are independent and the single weight function $\rho_3(\alpha, \mathbf{z})$ is sufficient to describe the sum of all relevant Feynman diagrams.

Further analysis of this vertex function gives various constrains on the integration regions α, \mathbf{z} , dependent on masses of the particles. For instance, for the $\Phi\Phi\phi$ interaction and m (μ) being the mass of particle Φ (ϕ), Eq. (37) reduces to the following two-variable spectral representation:

$$\Gamma(p, P) = \int_0^\infty d\alpha \int_{-1}^1 dz \frac{\rho(\alpha, z)}{\alpha - (p + z\frac{P}{2})^2 - i\epsilon} \quad (38)$$

in the region $0 < P^2 < 4m^2$, $P = p_1 + p_2$, $p = p_1 - p_2$. The spectral function $\rho(\alpha, z)$ is a positive regular function of the spectral variables for the fixed value of P^2 . Furthermore, if the internal lines with momenta p_1 and p_2 correspond to the particle Φ and the third external line corresponds to the particle ϕ , the following support of $\rho(\alpha, z)$ can be derived:

$$\rho(\alpha, z) = 0, \quad \text{unless} \quad \alpha > \left(m + \mu - (1 - |z|) \frac{\sqrt{P^2}}{2} \right)^2. \quad (39)$$

This two variable representation was first proposed in an axiomatic field theory [28],[29] and successfully used to solve the Bethe-Salpeter equation in various approximations [30],[31]. The paper [32] solves both the bound state equation and the scattering problem and applies this two variable representation to QED even in the nonperturbative regime.

The scattering matrix $M(p, q; P)$ describes the process $\Phi_1\Phi_2 \rightarrow \Phi_3\Phi_4$, where $p = q_1 - q_2$ and $q = q_3 - q_4$ are the initial and final relative momenta, respectively, and P is the total four-momentum. It is given by the infinite series of Feynman diagrams. The full renormalized scattering matrix can formally be written as [27]:

$$\begin{aligned} M(p, q; P) = & \int_0^\infty d\gamma \int_\Omega d\xi \left\{ \frac{\rho_{st}(\gamma, \xi)}{\gamma - [\sum_{i=1}^4 \xi_i q_i^2 + \xi_5 s + \xi_6 t] - i\epsilon} \right. \\ & + \frac{\rho_{tu}(\gamma, \xi)}{\gamma - [\sum_{i=1}^4 \xi_i q_i^2 + \xi_5 t + \xi_6 u] - i\epsilon} \\ & \left. + \frac{\rho_{us}(\gamma, \xi)}{\gamma - [\sum_{i=1}^4 \xi_i q_i^2 + \xi_5 u + \xi_6 s] - i\epsilon} \right\}, \quad (40) \end{aligned}$$

where q_i^2 is the square of the four-momentum carried by Φ_i and s, t , and u are the Mandelstam variables. Since only six of these variables are independent (due to the relation $q_1^2 + q_2^2 + q_3^2 + q_4^2 = s + t + u$), this is also the number of independent ξ -parameters. Hence, one only has to introduce the “mass” parameter γ and six dimensionless Feynman parameters ξ_i with one constraint. The symbol Ω denotes the integration region of ξ such that $\Omega = \{\xi | 0 < \xi_i < 1, \sum \xi_i = 1 (i = 1, \dots, 6)\}$. The function ρ_{ch} gives the weight of the spectrum arising from the different channels which can be denoted by $ch = \{st\}, \{tu\}, \{us\}$. Since any Feynman diagram for the scattering matrix can be written in this form, it must be also true for their sum. From the corresponding SDEs of considered theory it simply follows that PTIR for M must contain the weights of lower point Green’s functions. For instance, the simplest contribution from t -channel is given by a free propagator

$$M(p, q; P) = \frac{g^2}{m_{exch}^2 - (p - q)^2 - i\epsilon}, \quad (41)$$

and the corresponding weight is simply a product of six delta functions.

The first topologically less trivial diagrams are various boxes and crossed-boxes. Collecting various couplings to the constant prefactor C then the two-variable expression for crossed box diagram was derived some time ago by Mandelstam [18]:

$$\begin{aligned} I_{cross} &= C \int_{4\mu^2}^{\infty} \int_{4m^2}^{\infty} \frac{dt'}{t' - t - i\epsilon} \frac{du'}{u' - u - i\epsilon} \frac{\theta(\kappa(u', t'))}{\sqrt{\kappa(u', t')}} , \\ \kappa(u', t') &= u't' [(t' - 4\mu^2)(u' - 4m^2) - 4\mu^4] , \end{aligned} \quad (42)$$

where μ is mass of the exchanged particle ϕ (its propagators cross inside the diagram), while m is a mass of the scattered particle (emitting and absorbing ϕ). Here, the function

$$\sigma(u', t') = C \frac{\theta(\kappa(u', t'))}{\sqrt{\kappa(u', t')}} , \quad (43)$$

is called the double spectral function. It can be easily converted to the PTIR form:

$$I_{cross} = \int_0^{\infty} d\alpha \int_0^1 dz \frac{\rho_{ut}(\alpha, z)}{\alpha - zu - (1 - z)t} , \quad (44)$$

with the help of the Feynman identity.

3 SDEs and Unitary Equations in the scalar toy model

This Section should serve as a pedagogical introduction to the more general strategy of Unitary Equations. As we will see, using the spectral decomposition of GFs in SDEs allows to derive a real nonsingular integral equation for a real spectral function σ . For this purpose we consider a simple quantum model describing the self-interaction of one real spinless field ϕ . The Lagrangian density for our toy model reads

$$\mathcal{L} = \frac{1}{2} \partial_\mu \phi_0(x) \partial^\mu \phi_0(x) - \frac{1}{2} m_0^2 \phi_0^2(x) - g_0 \phi_0^3(x) + \lambda_0 \phi_0^4(x) + \dots , \quad (45)$$

where the subscript 0 indicates the unrenormalized quantities and the dots mean the neglected interactions with neglected field content.

The main philosophy of the derivation does not depend on the details of a given model. The method can be directly applied to all theories where the dispersion relation approach is accessible. We also explain and review the spectral technique used in the calculations of relativistic bound states in the subsequent Section. For this purpose we follow the main ideas of the paper [31] where the (massive and gauged) Wick-Cutkosky model and its response on electromagnetic interaction was considered. Furthermore, we not only exhibit the appropriate derivation of Unitary Equations but we also present the numerical solution and we offer the comparison with the results obtained via usual Euclidean formalism.

Using the diagrammatic representation for the selfenergy the SDE for scalar propagator G can be depicted as:

$$G_0^{-1}(p^2) = p^2 - m_0^2 - \Pi_0(p^2), \quad (46)$$

$$\Pi_0(q^2) = \text{---} \text{---} \text{---} + \text{---} \text{---} \text{---} + \text{---} \text{---} \text{---} + \text{---} \text{---} \text{---}, \quad (47)$$

where the full irreducible vertex functions $\Gamma_0^{[3]}$ ($\Gamma_0^{[4]}$) are represented by blobs (diamond) and they satisfy their own SDEs (for the derivation of SDEs from the effective action see some standard textbook, e.g. [33], but also [34]). All the internal lines stand for G , i.e. for fully dressed propagators. For the explanatory simplicity we neglect the two loops diagram, how to take into account the last two diagrams will be explained at the end of this Section. In our simple approximation the selfenergy to be considered is given by the first two diagrams above. Their contribution is:

$$\Pi_0(p^2) = i\lambda \int \frac{d^4q}{(2\pi)^4} G_0(q) + i3g_0 \int \frac{d^4q}{(2\pi)^4} \Gamma_0^{[3]}(p-q, q) G_0(p-q) G_0(q). \quad (48)$$

Furthermore, we approximate the trilinear and quartic vertices by their tree value: $\Gamma^{[3]} = 3!g$ and $\Gamma^{[4]} = 4!\lambda$ (note, contrary to the usual convention used in QED, we very naturally include the coupling constants into the definition of proper GFs). In such approximation the quartic interaction $\lambda\Phi^4$ as well as the field do not need renormalization since we have neglected higher diagrams. Thus the divergent integral defining Π_0 requires only the mass renormalization:

$$\Pi_R(\zeta; p^2) = \Pi_0(p^2) - \Pi_0(\zeta), \quad (49)$$

where the divergence (quadratic here) is absorbed to the counterterm part of the Lagrangian:

$$m_0^2 = m^2(\zeta) + \delta m^2, \quad \delta m^2 = \Pi_0(\zeta). \quad (50)$$

The renormalized equation for the propagator then reads

$$G^{-1}(p^2) = p^2 - m(\zeta)^2 - \Pi_R(\zeta; p^2),$$

$$\Pi_R(\zeta; p^2) = \Pi(p^2) - \Pi(\zeta), \quad (51)$$

$$\Pi(p^2) = i3g \int \frac{d^4q}{(2\pi)^4} \Gamma^{[3]} G(p-q) G(q), \quad (52)$$

where we have omitted the seagull diagram contribution in expression for $\Pi(p^2)$ since it exactly vanishes after the subtraction and where we simply take $G_0(p^2) = G(p^2)$ since the field strength renormalization constant $Z = 1$ here (for more complete discussion of the multiplicative renormalization in scalar models see the paper [35]).

The key point of our spectral technique is the derivation of the Unitary Equations. The Unitary Equations relate the imaginary part of the propagator -the spectral function σ - with the imaginary and the real part of proper GF (this is the reason why we call them the Unitary Equations). Dealing with explicitly massive model here, the generic spectral decomposition of the renormalized propagator (10) is used, where the spectral function of the stable particle is

$$\bar{\sigma}(\alpha) = r\delta(m^2 - \alpha) + \sigma(\alpha). \quad (53)$$

When propagator SR is used in the equation for Π Eq. (52) it leads to the DR for the renormalized selfenergy $\Pi_R(\zeta; p^2)$. Its form is well known from the perturbation theory treatment and is given by the DR already discussed in the Section 3. However here, for purpose of convenience of the reader and in order to make our explanation self-contained, we also give the appropriate derivation here.

Substituting SR for propagators into (51) the selfenergy Π reads

$$\begin{aligned} \Pi(p^2) &= 18g^2 \int d\alpha d\beta \bar{\sigma}(\alpha) \bar{\sigma}(\beta) I(p^2), \\ I(p^2) &= i \int \frac{d^4l}{(2\pi)^4} \frac{1}{((p+l)^2 - \alpha + i\epsilon)(l^2 - \beta + i\epsilon)}. \end{aligned} \quad (54)$$

Clearly $\Pi_R(\zeta; p^2)$ is given by the integral over the analogically defined $I_R(\zeta; p^2) = \Pi(p^2) - \Pi(\zeta)$. Using the Feynman parameterization I_R can be written as

$$\begin{aligned} I_R(\zeta; p^2) &= \int_0^1 dx \int \frac{d^4l}{(2\pi)^4} \left\{ \frac{i}{[l^2 + p^2x(1-x) - \alpha(1-x) - \beta x + i\epsilon]^2} - (p^2 \rightarrow \zeta) \right\} \\ &= \int \frac{d^4l}{(2\pi)^4} \int_0^1 \frac{-2i dx dz (p^2 - \zeta)x(1-x)}{[l^2 + (p^2 - \zeta)x(1-x)z + \zeta x(1-x) - \alpha(1-x) - \beta x + i\epsilon]^3} \\ &= \int_0^1 dx \frac{dz}{z} \frac{(4\pi)^{-2} (p^2 - \zeta)}{p^2 - \Omega + i\epsilon}, \end{aligned} \quad (55)$$

where we have labeled $\Omega = \zeta + \frac{-\zeta + \alpha/x + \beta/(1-x)}{z}$. Making a substitution $z \rightarrow \omega$ such that $\omega = \Omega$, it yields

$$I_R(\zeta; p^2) = \frac{1}{(4\pi)^2} \int_0^1 dx \int_{\frac{\alpha}{x} + \frac{\beta}{1-x}}^{\infty} \frac{p^2 - \zeta}{(p^2 - \omega + i\epsilon)(\omega - \zeta)}. \quad (56)$$

Changing the ordering of the integrations (note, the variables α, β are positive) and putting I into II we obtain the desired DR:

$$\Pi_R(\zeta; p^2) = \int_0^\infty d\omega \frac{\rho(\omega) \left[\frac{p^2 - \zeta}{\omega - \zeta} \right]^n}{p^2 - \omega + i\epsilon}, \quad (57)$$

where $n = 1$ here (while $n = 2$ when the field renormalization enters the calculation and the second subtraction is required, here we use n for general purpose) and where the absorptive part $\pi\rho$ is given as

$$\begin{aligned} \rho(\omega) &= C_g \int d\alpha d\beta \bar{\sigma}(\alpha) \bar{\sigma}(\beta) \frac{\lambda^{1/2}(\alpha, \beta, \omega)}{\omega} \Theta(\omega - (\sqrt{\alpha} + \sqrt{\beta})^2) \\ &= C_g r^2 \sqrt{1 - \frac{4m^2}{\omega}} \Theta(\omega - 4m^2) + \dots, \end{aligned} \quad (58)$$

where λ is the Khallen triangle function defined in (24) and the dots means the terms with one or two σ 's. (Thorough this paper we always use the letter ρ to denote the weight function that appears in selfenergy in order to carefully distinguish from the spectral function σ , i.e. from $\text{Im}G(p^2)/\pi$). C_g is used to label the coupling strength defined as $C_g = \frac{18g^2}{(4\pi)^2}$.

The derivation of Unitary Equations is achieved by using the functional identity

$$\frac{1}{x' - x + i\epsilon} = P. \frac{1}{x' - x} - i\pi\delta(x' - x), \quad (59)$$

where $P.$ denotes the principal value integration. $GG^{-1} = 1$ can be written as:

$$\left[\frac{r}{p^2 - m^2} + \int_{4m^2}^\infty d\alpha \frac{\sigma(\alpha)}{p^2 - \alpha - i\epsilon} \right] \left[p^2 - m^2(\zeta) - \int d\omega \frac{\rho(\omega) \left[\frac{p^2 - \zeta}{\omega - \zeta} \right]^n}{p^2 - \omega + i\epsilon} \right] = 1, \quad (60)$$

we arrive at the equations between the spectral functions σ and ρ and their principal values integral. We eliminate the unpleasant (since unknown) principal value integral over the function σ from the equation for the real part

$$\begin{aligned} P. \int d\omega \frac{\sigma(\omega)}{p^2 - \omega} &= \frac{1 - \pi^2 \rho(p^2) \sigma(p^2)}{b(p^2)} - \frac{r}{p^2 - m^2}, \quad (61) \\ b(p^2) \equiv \text{Re}G^{-1}(p^2) &= p^2 - m^2(\zeta) - P. \int d\omega \frac{\rho(\omega) \left[\frac{p^2 - \zeta}{\omega - \zeta} \right]^n}{p^2 - \omega}. \end{aligned}$$

The equation for imaginary part of Eq. (60) can be written as

$$\sigma(p^2) b(p^2) - \rho(p^2) \left(\frac{r}{p^2 - m^2} + P. \int d\omega \frac{\sigma(\omega)}{p^2 - \omega} \right) = 0. \quad (62)$$

Substituting (61) into the Eq. (62) we arrive at the desired Unitary Equation:

$$\sigma(p^2) = \frac{\rho(p^2)}{b^2(p^2) + \pi^2 \rho^2(p^2)}, \quad (63)$$

as follows from the rel. (58), the continuous spectral function σ starts to be smoothly nonzero from the perturbative threshold $4m^2$. Note that the function b still contain the principal value integral this can be evaluated numerically [35] in general, but in simple one loop case here it is known analytically. The form of the Eq. (63) is based only on the analytic property of the propagator, it does not depend on a details of interaction. All the dynamical information is contained in the expression for ρ which follows from the SDEs solution here, or from the usual Feynman diagram in the case of perturbation theory treatment. At the end we should mention that the derivation of Unitary Equations has been performed for momentum subtraction scheme only for simplicity. It should be stressed here, that the extension to any other renormalization scheme is very straightforward. Remind the changes in DR which arise due to finite change in the field renormalization constant Z . It would be reflected by the presence of nontrivial subtracting polynom before the DR (35). This can be easily incorporated into the Unitary Equations.

If the pole is assumed in the propagator then the knowledge of the pole mass m is required in the presented spectral treatment. From its definition $G^{-1}(m^2) = 0$ we can obtain the following equation

$$m^2 = m^2(\zeta) + \int d\omega \frac{\rho(\omega)}{m^2 - \omega} \left[\frac{m^2 - \zeta}{\omega - \zeta} \right]^n. \quad (64)$$

The propagator residuum can be obtained by the on-shell differentiation:

$$r = \lim_{p^2 \rightarrow m^2} \frac{p^2 - m^2}{p^2 - m^2(\zeta) - \Pi(\zeta; p^2)} = \frac{1}{1 + \int d\omega \frac{\rho(\omega)}{(\omega - m^2)^2}}. \quad (65)$$

3.1 Comparison with the Euclidean solution

It is instructive to compare our Minkowski-space result with the one obtained in Euclidean approach. For this purpose we consider the propagator SDE truncated and renormalized as before.

After the Wick rotation and angular β , ϕ integrations of the four-dimensional sphere

$$\int d\Omega_4 = \frac{1}{2\pi^2} \int_0^\pi d\theta \sin^2(\theta) \int_0^\pi d\beta \sin(\beta) \int_0^{2\pi} d\phi, \quad (66)$$

the renormalized SDE for propagator becomes

$$\Pi(x) = m^2(0) - \frac{2C_g}{\pi} \int_0^\infty dy \int_0^\pi d\theta \frac{\sin^2(\theta)y}{y + \Pi(y)} \left[\frac{1}{z + \Pi(z)} - \frac{1}{y + \Pi(y)} \right], \quad (67)$$

where we made subtraction at zero renormalization scale $\zeta = 0$. For purpose of brevity we have defined $\Pi(y) = \Pi_R(y = p_E^2; \zeta = 0) + m^2(0)$, variables x, y, z are squares of Euclidean momenta such that $z = x + y - 2\sqrt{xy} \cos \theta$

In our numerical treatment we put $m^2(0) = 1$ in arbitrary units. The coupling strength C_g is then scaled through the dimension-full coupling constant g which is taken in the units of $m(0)$.

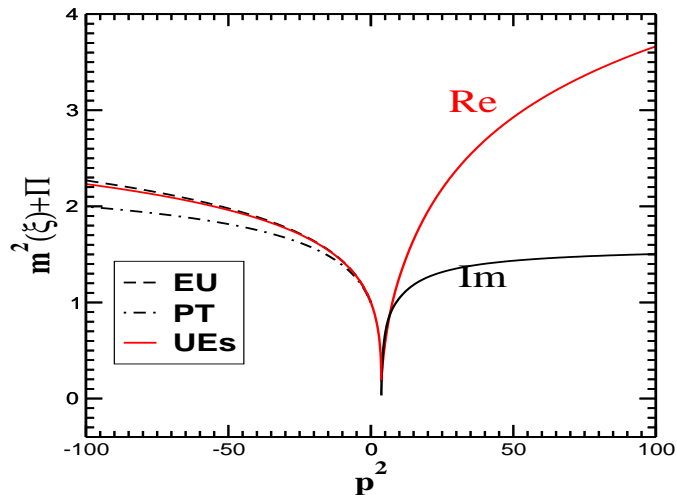


Figure 2. The renormalized mass plus selfenergy for the coupling strength $C_g = \frac{18g^2}{(4\pi)^2} = 0.5m^2(0)$. Minkowski result is labeled by Unitary Equations, EU stands for the solution of Euclidean SDE, PT means one loop perturbation theory.

Within the same choice of renormalization scale ζ and the same choice of renormalized mass the Minkowski problem has been solved to. The resulting 'total selfenergy' function $\Pi_R(p^2; 0) + m^2(0)$ is plotted in Fig. 2 for the coupling strength $C_g = 0.5m^2(0)$. The Unitary Equations as well as the Eq. (67) has been solved by the iterations without some peculiar troubles. We use Gaussian quadrature method for the integration. Note only that in order to calculate $\Pi(z_i)$ in (67) we need to interpolate (extrapolate) between the 'fitted' points $\Pi(x_i)$. To achieve good numerical accuracy in the Minkowski approach we have found it is necessary to use relatively large number of mesh points. This is a consequence of the presence of Heaviside step functions in the kernel and we take 800 of mesh points in the case of figure's calculation. The value of obtained physical mass is $m^2 = 0.92m^2(0)$ for $C_g = 0.5m^2(0)$. Furthermore, we compare with the one loop perturbation theory. These results are calculated with the physical pole mass as it has been determined from Unitary Equations. Note that determining pole mass from Eq. (64) in a framework of perturbation theory would lead to the small negligible shift of pole mass and threshold as well.

3.2 The relativistic bound-states

In quantum field theory the two body bound state is described by the bound state vertex function or, equivalently, by Bethe-Salpeter amplitudes, both of them are solutions of the corresponding (see Fig. 3) covariant four-dimensional Bethe-Salpeter equation [36]. In the so-called ladder approximation the scattering matrix is given by the sum of the generated ladders. When the more realistic models are considered (hadronic physics for example) one is forced to use dressed

correlation functions instead of their bare approximations.

Here we are considering simple super-renormalizable model with cubic interaction $\phi_i^2\phi_3; i = 1, 2$ of three massive fields (thus this model can be called massive Wick-Cutkosky model), where in the approximation that allows us to exploit the results of previous Section. Having the propagators calculated within the bare vertex truncation of the SDEs we combine them with the dressed ladder approximation for the scalar s-wave bound state amplitudes. To do this explicitly we follow the treatment described in [31] where the spectral technique was used to obtain the accurate results directly in Minkowski space. In the mentioned paper the analytic formula has been derived for the resulting equation which significantly simplify the numerical treatment. For the extensive but certainly not exhaustive review of up to date known or used methods in scalar models see also [31].

For our purpose we utilize the PTIR already reviewed in the Section 3. Very similar to the SDEs treatment reviewed in the previous Sections, here the Bethe-Salpeter equation written in momentum space is converted into a real integral equation for a real weight function. This then allows us to treat the ladder Bethe-Salpeter equation in which all propagators (of constituents and of the exchanged particle) are fully dressed. This is achieved by the implementation of SR of the propagator which is determined by the appropriate set of SDEs. Having solved equations for spectral functions, one can easily determine the Bethe-Salpeter amplitudes in an arbitrary reference frame.

3.3 Solution of Bethe-Salpeter equation in Minkowski space

The Bethe-Salpeter amplitude for bound state (ϕ_1, ϕ_2) in momentum space is defined through the Fourier transform of

$$\langle 0|T\phi_1(x_1)\phi_2(x_2)|P\rangle = e^{-iP\cdot X} \int \frac{d^4p}{(2\pi)^4} e^{-ip\cdot x} \Phi(p, P), \quad (68)$$

where $X \equiv \eta_1 x_1 + \eta_2 x_2$ and $x \equiv x_1 - x_2$, so that $x_1 = X + \eta_2 x$, $x_2 = X - \eta_1 x$. Here $p_{1,2}$ are the four-momenta of particles corresponding to the fields $\phi_{1,2}$ that constitute the bound state (ϕ_1, ϕ_2) . The total and relative momenta are then given as $P = p_1 + p_2$ and $p = (\eta_2 p_1 - \eta_1 p_2)$, respectively, and $P^2 = M^2$, where M is the mass of the bound state. Finally, $P \cdot X + p \cdot x = p_1 \cdot x_1 + p_2 \cdot x_2$. From now on we will put $\eta_1 = \eta_2 = 1/2$ for simplicity.

Introducing the scalar Bethe-Salpeter vertex function $\Gamma = iG_1^{-1}G_2^{-1}\Phi$, the homogeneous Bethe-Salpeter equation for a s-wave bound state reads

$$\Gamma(p, P) = i \int \frac{d^4k}{(2\pi)^4} V(p, k; P) G_1(k + P/2) G_2(-k + P/2) \Gamma(k, P). \quad (69)$$

The bound states appear as poles of the scattering matrix at total momenta $0 \leq P^2 < (m_1 + m_2)^2$ from which the constrain on the normalization condition follows (for the derivation see for instance [35]).

In the original Wick-Cutkosky model [37] the exchanged boson is massless in the kernel V and no radiative corrections are considered. This model is particularly interesting because it is the only example which is solvable exactly [37].

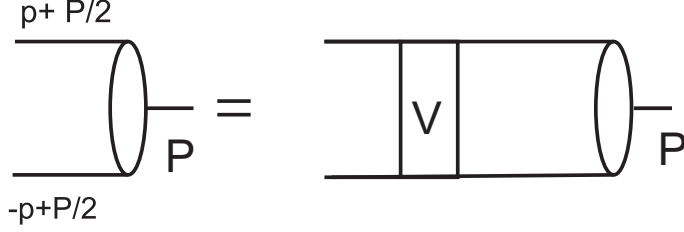


Figure 3. Diagrammatic representation of the Bethe-Salpeter equation for the bound state vertex function.

For this model the s-wave bound state the PTIR reduces to the one dimensional expression:

$$\Gamma(p, P) = \int_{-1}^1 dz \frac{\rho(z)}{m^2 - (p^2 + zp \cdot P + P^2/4) - i\epsilon}, \quad (70)$$

where the function $\rho(z)$ satisfies the equation

$$\begin{aligned} \rho(z') &= \frac{g^2}{(4\pi)^2} \int_{-1}^1 dz V^{[1]}(z', z) \rho(z), \\ V^{[1]}(z', z) &= \sum_{s=\pm} \frac{\Theta(s(z-z')) T_s}{2(m^2 - S)}, \\ S &= \frac{1-z'^2}{4} P^2 \quad ; \quad T_{\pm} = \frac{1 \pm z'}{1 \pm z}. \end{aligned} \quad (71)$$

The resulting weight functions $\rho(z)$ for various fraction of binding $\eta = \sqrt{P^2}/2m$ are displayed in Fig. 4.

When the mass of exchanged particle is nonzero or even when the other diagram is considered in the kernel of Bethe-Salpeter equation then the appropriate PTIR for the Bethe-Salpeter vertex function is two dimensional [27] (see also(38))

$$\Gamma(p, P) = \int_{-1}^1 dz \int_{\alpha_{min}(z)}^{\infty} d\alpha \frac{\rho^{[n]}(\alpha, z)}{[\alpha - (p^2 + zp \cdot P + P^2/4) - i\epsilon]^n}. \quad (72)$$

Thus the equation for original Wick-Cutkosky model is regarded as only the special case of (72) where the weight factorizes and is singular in α . However here, all the particles are massive thus the positive integer n represents a dummy parameter constrained only by convergence of the solution. The choice $n = 2$ was found to be a reasonable one.

In this case the Bethe-Salpeter equation can be converted to the following real integral equation for the real spectral function:

$$\rho^{[2]}(\alpha', z') = \frac{g^2}{(4\pi)^2} \int_{-1}^1 dz \int_{\alpha_{min}(z)}^{\infty} d\alpha V^{[2]}(\alpha', z'; \alpha, z) \rho^{[2]}(\alpha, z), \quad (73)$$

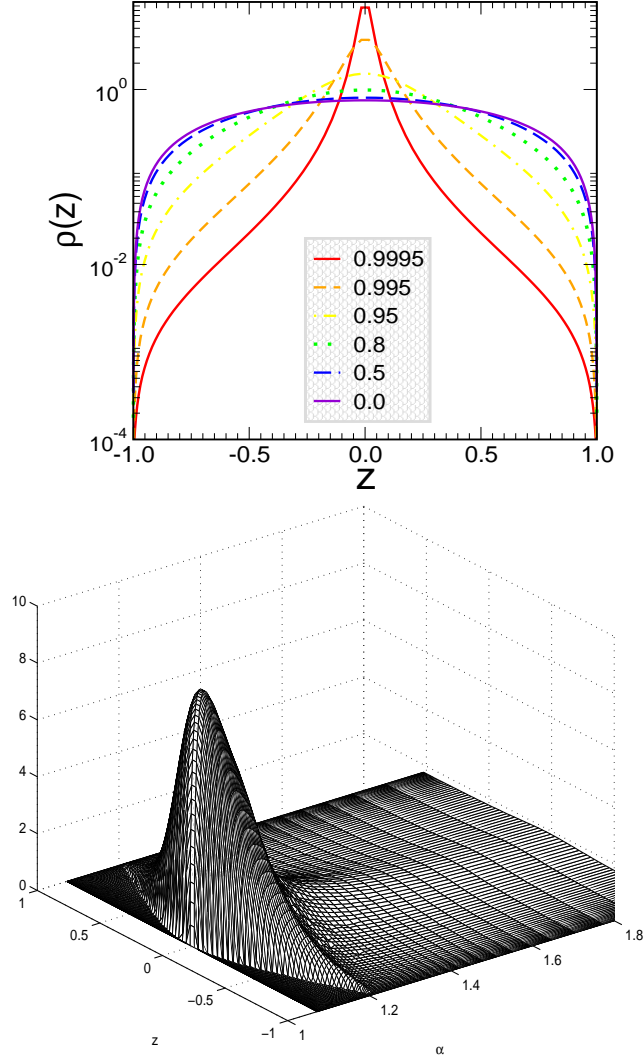


Figure 4. Top figure displays the weight function $\rho(z)$ in the original Wick-Cutkosky model ($m_3 = 0$) for several values of $\eta = \sqrt{P^2}/2m$. The Bottom figure displays rescaled weight function in the massive Wick-Cutkosky model for $m_3 = 0.1m$ and $\eta = 0.95$.

The interaction kernel is $V(p, k; P) = g^2 G_3(p - k)$ in the dressed ladder approximation, where all the propagators are understood to be fully dressed. For this case the kernel in spectral Eq. (73) $V^{[2]}(\alpha', z'; \alpha, z)$ has been derived in [31]. The explicit formula reads

$$V^{[2]}(\alpha', z', \alpha, z) = \sum_T \prod_{j=1}^3 \int d\alpha_j \bar{\sigma}(\alpha_j) \sum_{i=\pm} \frac{\theta(x_i) \theta(1-x_i) \theta(D)}{2J(\alpha, z)^2} \left\{ \frac{TJ(\alpha, z)}{(1-x_i)|E(x_i, S, \alpha')|} - \text{sgn}(E(x_i, S, \alpha')) \ln(1-x_i) \right\}_{x_i=x_i(T)}, \quad (74)$$

where the functions entering the above relation are

$$\begin{aligned}
x_{\pm}(T) &= \frac{\alpha' - \alpha_3 - R_T \pm \sqrt{D}}{2(\alpha'_S)}, \\
D &= (R_T - \alpha' + \alpha_3)^2 - 4\alpha_3(R_T - S), \\
E(x_{\pm}, S, \alpha') &= \alpha' - \frac{\alpha_3}{x_{\pm}^2} - S, \\
R_T &= J(\alpha, z)T + \frac{\alpha_1 + \alpha_2}{2} + \frac{\alpha_1 - \alpha_2}{2} z', \\
J(\alpha, z) &= \alpha - \frac{\alpha_1 + \alpha_2}{2} - \frac{\alpha_1 - \alpha_2}{2} z,
\end{aligned} \tag{75}$$

and where the symbol \sum_T should be understood as

$$\sum_T f(T) = f(0) - \theta(z - z')f(T_+) - \theta(z' - z)f(T_-), \tag{76}$$

where f is an arbitrary function.

The spectral function $\bar{\sigma}_i$ in Eq. (74) corresponds with the SR of i-particle propagator of i-field in the considered and relevant part of the Lagrangian

$$\mathcal{L}_{(strong)} = -g\phi_1^+ \phi_1 \phi_3 - \frac{g}{2} \phi_2^2 \phi_3. \tag{77}$$

These were obtained from the Unitary Equations. Note that $n = 2$ in DRs (57) because of two subtractions were made, i.e.

$$\Pi_{iR}(p^2) = \Pi_i(p^2) - \Pi_i(\zeta) - (p^2 - \zeta_i) \frac{d\Pi_i(p^2)}{dp^2} \Big|_{p^2=\zeta_i}, \tag{78}$$

since the on-shell renormalization prescription $\zeta_i = m_i^2$ with unit residuum was chosen.

The derivation of DRs for all three Π_{iR} is very straightforward and follows the lines of previous Section (for some details see [31]). The absorptive part of Π is given by ρ_i/π , these are

$$\begin{aligned}
\rho_i(\omega) &= \frac{g^2}{(4\pi)^2} \int d\alpha d\beta X(\alpha, \beta; \omega) \bar{\sigma}_3(\alpha) \bar{\sigma}_i(\beta), \quad i = 1, 2, \\
\rho_3(\omega) &= \frac{g^2}{(4\pi)^2} \sum_{i=1,2} \int d\alpha d\beta X(\alpha, \beta; \omega) \bar{\sigma}_i(\alpha) \bar{\sigma}_i(\beta),
\end{aligned} \tag{79}$$

where X is defined by Eq. (24).

In the ladder approximation the obtained spectrum agree with the one obtained by other techniques [38, 30, 39, 40]. In dressed ladder approximation there is no other reliable result published in literature to be compared with. However the qualitative agreement with the paper [39] was found: The critical value of coupling constant g_c (defined by the constraint for the renormalization constant: $Z(g_c) = 0$) as it has read from SDEs gives the physical domain of applicability of Bethe-Salpeter equation.

It is interesting to note here that within the use of Feynman-Schwinger representation method there was found in [41] that the crossed boxes are dominates in scalar models studied here. For a comparison of different technique, including Bethe-Salpeter see the result in this paper. The observed dumping of bound state energy is due to the bose statistic of the matter field in the model considered here (while there is an expected cancellation between higher order skeletons when one consider the bound states of fermions).

At this place we should mention the so called 'ghost' solution of Bethe-Salpeter equation. These, probably unphysical solutions (see [39] and references therein), have been found only for rather strong coupling in ladder approximation. However, the couplings below the critical one allow only solutions for relatively weakly bound states and neither 'ghost' solution of the Bethe-Salpeter equation was found. It suggests the domain of validity of SDEs restricts the solutions of the Bethe-Salpeter equation in such way that only the normal solutions exist.

3.4 Elastic Electromagnetic Form Factor

Although the elastic form factor represents a simple dynamical observable, its Minkowski calculation represents a nontrivial task. For this purpose we consider the massive Wick-Cutkosky model given by a Lagrangian gauged as follows:

$$\begin{aligned}\mathcal{L} &= (D^\mu\phi_1)^\dagger D_\mu\phi_1 + \frac{1}{2}\partial_\mu\phi_2\partial^\mu\phi_2 + \frac{1}{2}\partial_\mu\phi_3\partial^\mu\phi_3 - \frac{1}{4}F_{\mu\nu}F^{\mu\nu} - V(\phi_i), \\ V(\phi_i) &= (m_1^2 + g\phi_3)\phi_1^\dagger\phi_1 + \left(\frac{m_2^2}{2} + \frac{g}{2}\phi_3\right)\phi_2^2 + \frac{1}{2}m_3^2\phi_3^2,\end{aligned}\quad (80)$$

where the covariant derivative is $D_\mu = \partial_\mu - ieA_\mu$.

The electromagnetic form factors parametrize the response of bound systems to external electromagnetic field. The calculation of these observables within the Bethe-Salpeter framework proceeds along the Mandelstam's formalism [42]. In the form factor calculations the effects of scalar dressing were not taken into account.

The current conservation implies the parametrization of the current matrix element G^μ in terms of the single real form factor $G(Q^2)$

$$G^\mu(P_f, P_i) = G(Q^2)(P_i + P_f)^\mu, \quad (81)$$

where $Q^2 = -q^2$, so that Q^2 is positive for elastic kinematics.

The matrix element of the current in relativistic impulse approximation is depicted in Fig. 5. The matrix element is given in terms of the Bethe-Salpeter vertex functions as

$$\begin{aligned}G^\mu(P + q, P) &= i \int \frac{d^4p}{(2\pi)^4} \bar{\Gamma}(p + \frac{q}{2}, P + q) \\ &[D(p_f; m_1^2)j_1^\mu(p_f, p_i)D(p_i; m_1^2)D(-p + P/2; m_2^2)] \Gamma(p, P),\end{aligned}\quad (82)$$

where we denote $P = P_i$ and j_1^μ represents one-body current for particle ϕ_1 , which for the bare particle reads $j_1^\mu(p_f, p_i) = p_f^\mu + p_i^\mu$, where p_i, p_f is initial and final

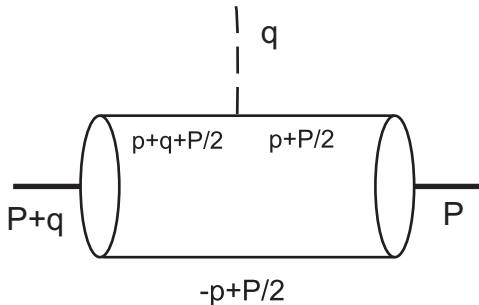


Figure 5. Diagrammatic representation of the electromagnetic current bound state matrix element.

momentum of charged particle inside the loop in Fig. 5, i.e., $p_i = p + P/2, p_f = q + p + P/2$.

The main result, as far as charge form factor is concerned, is the rewriting of the rhs of Eq. (82) directly in terms of the spectral weights of the bound state vertex function. It allows the evaluation of the form factor by calculating the dispersion relation:

$$G(Q^2) = \int d\omega \frac{\rho_G(\omega)}{Q^2 + \omega - i\epsilon} \quad (83)$$

without having to reconstruct the vertex functions $\Gamma(p, P)$ from their spectral representation. Unfortunately the derived expression for ρ_G in the DR (83) contains some additional integrations which the authors were not able to remove. Due to this and in order to avoid sizable numerical errors the results have been calculated only for positive Q^2 . However a dramatic and exciting changes can be expected at timelike momentum regime. This remained unexplored until now.

4 Strong coupling QED

In this Section we investigate SDEs in 3+1 dimensional QED. We follow the prospects presented in the papers [13, 14], in which the solution for this theory in Euclidean and Minkowski space were compared for the first time.

The first part of this Section is devoted to the solution for the electron propagator in ladder approximation, in the second part an extension to the unquenched case (with the photon polarization included) is made. In the latter case the running coupling is considered self-consistently: the fermion mass and photon polarization function have been calculated by solving the coupled SDEs for electron and photon propagators in Landau gauge. In this paper we do not use the vertex ansatz as in the paper [14] but we consider the first term of skeleton expansion (i.e. bare γ^μ vertex is used). Having small quantitative effect, because of Landau gauge, this not only drastically simplified the calculation effort but allows us to perform many integrations analytically. Likewise in the Section where we discuss a scalar model we write down the Unitary equations where the principal value integrations are excluded. This is a clear advantage when compared with earlier version of Unitary Equations [13, 14] where this possibility was overlooked.

In both approximations we are looking for solutions with zero and nonzero electron mass in Lagrangian. In the first case the chirally symmetric solution (with massless electrons) always exists. In the Euclidean formalism we obtained agreement with many previous studies [43, 44, 45], for sufficiently large coupling α also nontrivial solution for the mass function. On the other hand, no such solution was found in our spectral Minkowski approach. This is a strong indication that the dynamical fermion mass function has in this case a complicated (complex) structure, which is not reflected by assumptions of our spectral Ansatz.

We will be dealing mostly with the strong coupling regime, which is far from “real-life QED”, for which α_{QED} (in experimentally accessible energy region) is small and use of perturbation theory is fully justified. Of course, all our solutions agree in weak coupling limit with the perturbation theory.

As it is already stated in the introduction the basic motivation is to decode the timelike structure of nonperturbatively obtained Green’s functions. For this purpose the models considered here are an ideal playground. However, in this Section the reader can find at least two other reasons to consider strong-coupling QED dynamics.

The strong-coupling Abelian dynamics was considered as one of the candidates for explanation of electroweak symmetry breaking [46]. Such or a similar models can approximate the dynamics in the strong coupling sector in various Technicolors model, e.g., Slowly Walking Technicolors [47, 48, 49, 50], for which ladder approximation of QED-like theory seems to provide a test background for modeling of the (Techni)lepton propagators (for a possible indirect experimental evidence of Technicolor-like model see [51]). Moreover, the strong-coupling Abelian model is not only a suitable playground for studies of supercritical phenomena like dynamical mass generation, but it is suitable also for investigations of the analytical structure of the fermion propagator. It was 30 years ago when Fukuda and Kugo [52] observed the disappearance of the real pole of the fermion propagator in the ladder QED and it was argued that this is a signal for confinement of the fermion. Again, the main motivation is the simplicity of the model, in alternative more complicated models the nonperturbative phenomena are even more difficult to study quantitatively. We believe that it is worth reviewing the recent progress in strong coupling QED.

Our attention is mainly focused on the SDE for the fermion propagator, because no nontrivial nonperturbative effects (i.e. effects not known from perturbation theory) were found in the photon propagator. However, let us remind the solution of perturbation theory renormalization group equations for the running coupling [53], which in two loop approximations exhibits Landau singularity at the scale

$$\Lambda_L = m_R \exp \left[\frac{1}{\beta_1 e_R^2} \left(\frac{\beta_2 e_R^2}{\beta_1 + \beta_2 e_R^2} \right)^{\beta_2/\beta_1^2} \right]. \quad (84)$$

where β_i are the coefficients of QED beta function

$$\beta = \frac{e_R^3}{12\pi^2} + \frac{e_R^5}{64\pi^4} + \dots = \beta_1 e_R^3 + \beta_2 e_R^5 + \dots \quad (85)$$

$$\Gamma^\mu = \text{tree-level vertex} + \text{loop correction} \quad (99)$$

Figure 6. Diagrammatic representation of the Schwinger-Dyson equations for vertex function. Like in the diagrams for selfenergy the blobs (box) represent the exact vertex and the internal lines represent the exact propagators— wavy line stands for the photon and the straight line labels fermion propagator.

while the same implies transversality of the polarization tensor:

$$q_\nu \Pi^{\mu\nu}(q) = 0, \quad (92)$$

noting here that Eq. (92) also follows from Eq. (88) using Eq. (91) provided the divergent integrals in (88) are regularized by a translation invariant manner.

Therefore, in this case, the vacuum polarization tensor can be parameterized in terms of single scalar function $\Pi(q^2)$:

$$\Pi^{\mu\nu}(q) = q^2 \left[g^{\mu\nu} - \frac{q^\mu q^\nu}{q^2} \right] \Pi(q^2). \quad (93)$$

After the inversion, it yields for the photon propagator

$$G_{\mu\nu}(q) = -\frac{1}{q^2} \left[H(q^2) \left(g_{\mu\nu} - \frac{q_\mu q_\nu}{q^2} \right) + \xi_A \frac{q_\mu q_\nu}{q^2} \right], \quad (94)$$

where we define the photon renormalization function $H(q^2)$ as:

$$H(q^2) \equiv \frac{1}{1 - \Pi(q^2)}. \quad (95)$$

From (94) one finds that the bare photon propagator is given by:

$$G_{\mu\nu}^0(q) = -\frac{1}{q^2} \left[\left(g_{\mu\nu} - \frac{q_\mu q_\nu}{q^2} \right) + \xi_A \frac{q_\mu q_\nu}{q^2} \right]. \quad (96)$$

The general form for fermion propagator (89) is

$$S^{-1}(p) = A(p^2) p_\mu \gamma^\mu + B(p^2), \quad (97)$$

or alternatively:

$$S(p) = \frac{F(p^2)}{\not{p} - M(p^2)}, \quad (98)$$

where $F(p^2) = A^{-1}(p^2)$ is called the fermion wavefunction renormalization and $M(p^2) = B/A$ is the fermion mass function. Clearly the fermion propagator for a free fermion field or bare fermion propagator is given by $\Sigma = 0$ in Eq. (89).

4.2 Physical constraints on the solution

The model discussed in Section 3 was too simple and thus does not render some very important issues encountered when one deals with more realistic models, e.g. the models for which we use a gauge theory concept as a starting point. Therefore we discuss here the physical criteria which make the solution of SDEs (and any other nonperturbatively obtained solution of Green's functions) physically meaningful.

In Quantum Field Theory an experimental observable is given by the transition probability associated with the appropriate part of the S-matrix. When dealing with a renormalizable gauge theory the S-matrix element describing a given process should be completely independent on the renormalization scale (it is renormalization group invariant) and on the particular choice of gauge-fixing parameters (it is gauge-fixing independent). Furthermore – as shown above – the GFs should satisfy the Ward identities. For a sufficiently small coupling constant the usual perturbation theory in conventional gauges offers a safe way to satisfy all the required invariance. It is well known that the gauge variant (unphysical) parts usually involved in the original GFs cancel out in a given S-matrix element. To this end, there is recent progress in the so-called *Pinch Technique* [55, 56] which offers gauge-fixing independent Green's functions to all orders of perturbation theory both for the Abelian and nonAbelian case. It is also remarkable that similar to the *Background-Field Method* the Pinch Technique GFs automatically satisfy the naive Ward identities rather than more complicated Slavnov-Taylor identities.

The problem of gauge invariance in the nonperturbative SDEs formalism is not yet fully solved. Adopted techniques should maximally respect the gauge identities such as Ward identities, Nielsen identities [57] and Landau-Khalatnikov transformation [58, 59] when class of linear covariant gauges in QED is used. Clearly, the best we could have from this point of view is the systematic method of building the renormalized blocks of GFs which are already free of unphysical information. Very promising but rather complicated method is to circumvent the gauge fixing problem by the use of stochastic quantization. This unconventional idea is based on the introduction of a fifth stochastic-time coordinate, while the usual observables are obtained in the equilibrium. (The *stochastic quantization* and its relation to the usual methods is up to date exhaustively reviewed in [60]). Since contrary to the effective action approach here, this method does not require gauge fixing at all and hence it offers also the gauge fixing invariant GFs. Further, it is important to note that within the certain approximations the stochastic quantization yields the same Yang-Mills SDEs as conventional approach in Landau gauge [63]. The second promising method could be above mentioned Pinch Technique which was originally developed in the context of SDEs [61, 62] in 1980's. However, in this strategy the requirement of multiplicative renormalizability has been ignored and to the best of author's knowledge from that time no progress has been made in utilization of Pinch technique in the SDEs formalism.

The gauge technique [64, 65], being based on the spectral representation offers GFs satisfying Ward identity in the whole Minkowski space. Within the

context of gauge technique R. Delbourgo in Ref. [66] highlights some of the related problems hindering the studies of SDEs. Among these, the first one is how well the Green's function solutions obey the Landau-Khalatnikov transformation and the second is how closely do the nonperturbative answers coincide with the perturbation series if we expand them in the power of couplings.

Making a simple Ansatz for a gauge vertices one can ensure Ward identity irrespective of analytical properties of GF's. In QED the simplest solution is the Ball-Chiu vertex [67], while any improved Ansatz can differ at most in the transversal part of vertex function. For an exhaustive list of the modeling vertices in QED see the papers [68, 69]. However stressed here that the recent numerical study [70] of the gauge dependence of the chiral condensate leads us to the conclusion that the Ward identity alone is not sufficient to ensure the gauge independence of the physical observable. Further, it is argued that it is essential to apply full Landau-Khalatnikov transformation to the dynamically generated mass function as also advocated in [71]. This step seems to be necessary in order to obtain a reliable results in other gauges than Landau gauge.

With the exception of the gauge technique to solve the system of SDEs within the help of spectral technique means to calculate complicated formula which should lead to the evaluation of dispersion relation for proper GFs at the end. Therefore we instead considering some Ansatz for the vertex function we rather use the (two simplest) skeleton expansion of self-energies and our calculation is performed in conventional Landau gauge where $\xi_A = 0$. Such skeleton expansion can be systematically improved by considering further and further terms in the multiloop expansion. In agreement with the issues made in the paper [72] we assume that the usage of Landau gauge should lead to the approximately gauge invariant GFs and gauge-fixing independent observables.

The renormalizability means that divergences may be removed (order-by order in perturbation theory) upon the field redefinitions

$$\psi \rightarrow \sqrt{Z_2}\psi, \quad A_\mu \rightarrow \sqrt{Z_3}A_\mu, \quad (100)$$

and vertex renormalization

$$\gamma^\mu \rightarrow Z_1\gamma^\mu. \quad (101)$$

If the renormalization scheme respects the Ward-Takahashi identity, i.e.

$$Z_1 = Z_2 \quad (102)$$

in the exact theory we say that QED is *multiplicatively renormalizable*.

To summarize, we impose the physical criteria, which will allow one to determine the solution of SDEs to be physically meaningful (in general renormalizable gauge theory).

- The theory should be multiplicatively renormalizable, which implies:
 - the number of possible subtractions for a given GF (in momentum subtraction scheme).
 - the relation between various renormalization constants (and hence the coefficient of subtracting polynomials).

- renormalized GFs satisfy WTIs.
- various possible renormalization schemes are physically equivalent
- the position of the pole in the propagators is scheme-invariant.

In addition, for the theory to be tractable in our Minkowski approach the following is assumed or required

- The propagators are analytical functions in the whole complex plane of the momenta except the real positive axis, which implies:
 - the vertices satisfy integral representation known from perturbation theory (here it is assured by skeleton expansion of GFs)
 - the proper Green's functions satisfy dispersion relations

However, note here: neither the existence of a pole nor the positivity of the SR is needed.

4.3 Ladder approximation of electron SDE with nonzero bare mass

In ladder approximation the vacuum polarization is neglected: the photon propagator is taken in its bare form and the photon-fermion-fermion vertex is approximated by the pure γ^μ matrix. The relative technical simplicity of calculations in the ladder approximation for electron SDE is an attractive feature rendering very interesting study without some large computational effort. It allows transparent comparison with the Euclidean and the perturbation theory results as well.

Using bare vertex and bare photon propagator leads to the following ladder fermion SDE:

$$\begin{aligned} S^{-1}(p) &= Z_2[\not{p} - m_0] - \Sigma(p), \\ \Sigma(p) &= ie^2 \int \frac{d^4k}{(2\pi)^4} G_{free}^{\mu\nu}(k) \gamma_\mu S(p-k) \gamma_\nu. \end{aligned} \quad (103)$$

Further we introduce the mass renormalization constant Z_m and/or the mass counterterm δ_m

$$m_0 = Z_m m(\zeta); \quad \delta_m = m_0 - m(\zeta), \quad (104)$$

relating the renormalized mass $m(\zeta)$ at the renormalization scale ζ to the bare mass m_0 and recall that $Z_1 = Z_2 = 1$ in ladder approximation in Landau gauge.

4.4 Euclidean formulation

First of all, in order to make a careful and constructive comparison with the standard Euclidean results we review the basics of the standard Euclidean formulation [52, 43, 44] results presented in the literature. Taking the traces Tr and $Tr \not{p}$ in the first Eq. (103) the SDE is transformed into one equation for the mass $M_E = B_E$:

$$\begin{aligned} A_E(x) &= 1, \\ B_E(x) &= m_0 + \frac{3\alpha}{4\pi} \int_0^\infty dy K(x, y) \frac{B_E(y)}{y + B_E^2(y)}, \\ K(x, y) &= \frac{2y}{x + y + \sqrt{(x-y)^2}}, \end{aligned} \quad (105)$$

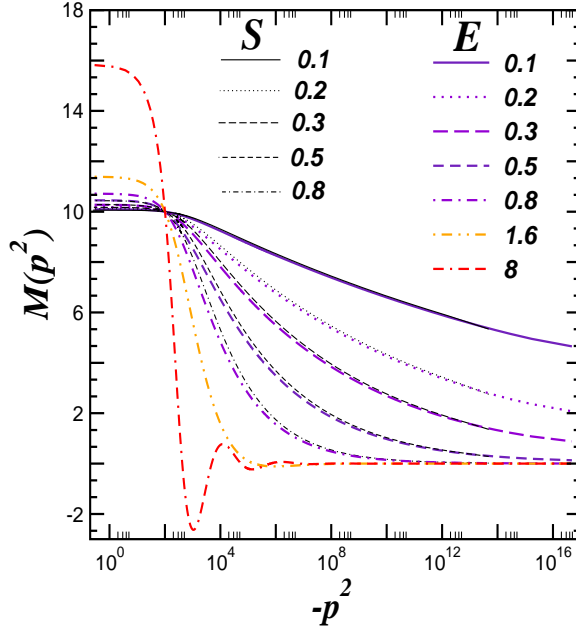


Figure 7. Spacelike solutions for mass function of the electron propagator as have been obtained within spectral (S) and Euclidean (E) formalism.

where Wick rotation and angle integration have been done and where we have used $Z_2 = 1$, $x \equiv p_E^2 = -p^2$, $y \equiv k_E^2 = -k^2$. The renormalized Eq. (105) then reads

$$B_E(\zeta, x) = m(\zeta) + \frac{3\alpha}{4\pi} \int_0^\infty dy V(\zeta, x, y) \frac{B_E(\zeta, y)}{y + B_E^2(\zeta, y)}, \quad (106)$$

$$V(\zeta, x, y) = K(x, y) - K(\zeta, y).$$

Recall here that Eq. (105) with zero bare mass ($m_0 = 0$) provides nontrivial solution only for $\alpha > \alpha_c$ (the so called supercritical QED, α_c is critical coupling) while $B(p^2) = 0$ for $\alpha < \alpha_c$ (chiral symmetric phase). Recall also here that the supercritical solution requires the implementation of a UV regulator Λ_H owing to Miransky scaling [73, 74]:

$$B(0) \simeq \Lambda_H \sqrt{1 - \frac{\alpha_c}{\alpha}}, \quad (107)$$

where Λ_H is the naive (translation invariance violating) integral momentum cut-off.

In this paper we solved the SDE (106) with the renormalization choice $M(\zeta = -10^2) = 10$. The results are displayed in Fig. 7. It is not surprising that for $\alpha > \alpha_c$ the obtained results do not agree with perturbation theory at all. In

agreement with the studies [52, 44] the expected damping of the mass function to its negative values is observed in supercritical phase of QED.

4.5 Minkowski formulation

As in the scalar theory discussed earlier, we use the SR for the propagator and arrive at DRs for selfenergy. Although the results of this Section are presented for ladder approximation QED the renormalization wave function A will be formally kept during the calculation for a possible more general future studies. There are two independent spectral functions in SR for QED fermion propagator:

$$S(p) = \int ds \frac{\not{p}\bar{\sigma}_v(s) + \bar{\sigma}_s(s)}{p^2 - s + i\varepsilon} = \frac{r}{\not{p} - m} + \int ds \frac{\not{p}\sigma_v(s) + \sigma_s(s)}{p^2 - s + i\varepsilon}, \quad (108)$$

where m is the physical electron mass. As usual the propagator is split into a real pole part and a part that is generated by the interactions. To avoid confusion from the beginning, it is stressed here that the assumption (108) does not imply (but does not exclude) real or complex pure pole singularity structure of the electron propagator. Thanks to the masslessness of the photon, the branch point corresponds to the physical mass of the electron. The gauge-dependent complex singularity appears after the limit $p^2 \rightarrow m_+^2$, while under the threshold $p^2 \rightarrow m_-^2$ the propagator is assumed to be a real function in any case. This known fact is reflected by the threshold behavior of the continuous spectral function $\sigma_{v,s}$ (in the previous scalar case the spectral function was zero at the threshold, however here $\sigma_{v,s}(m_-^2) \neq 0$ in general).

We split the unrenormalized self-energy (103) into its Dirac vector and Dirac scalar part

$$\Sigma(p) = \not{p} a(p^2) + b(p^2). \quad (109)$$

The self-energy in Eq. (103) is only logarithmically divergent and one subtraction:

$$a_R(\zeta; p^2) = a(p^2) - a(\zeta) = \int d\omega \frac{\rho_v(\omega)(p^2 - \zeta)}{(p^2 - \omega + i\varepsilon)(\omega - \zeta)}, \quad (110)$$

$$b_R(\zeta; p^2) = b(p^2) - b(\zeta) = \int d\omega \frac{\rho_s(\omega)(p^2 - \zeta)}{(p^2 - \omega + i\varepsilon)(\omega - \zeta)}. \quad (111)$$

is sufficient to renormalize the self-energy: $\Sigma_R(\zeta, p) = \not{p} a_R(\zeta; p^2) + b_R(\zeta; p^2)$, where two scalar functions a, b satisfy the DRs written also above.

Relatively straightforward calculations [13, 35] lead to the results for the imaginary parts of the functions (110),(111) with the result $\rho_v = 0$ while the weight function ρ_s reads

$$\rho_s(p^2) = -3 \left(\frac{e}{4\pi} \right)^2 \left[rm \left(1 - \frac{m^2}{p^2} \right) + \int_{m^2}^{p^2} d\alpha \sigma_s(\alpha) \left(1 - \frac{\alpha}{p^2} \right) \right] \Theta(p^2 - m^2). \quad (112)$$

As we already saw in the previous Section the peculiarity of the ladder approximation electron SDE in Landau gauge gives for the renormalization wave

function $A(\zeta; p^2) = 1 + a_R(\zeta; p^2) = 1$ and renormalization group invariant mass function is

$$M(p^2) = B(p^2) = m(\zeta) + b_R(\zeta; p^2). \quad (113)$$

The Unitary equations can be most easily derived from the following identity

$$S^{-1}S = 1, \quad (114)$$

where we use the SR (108) to express fermion propagator S and SDE in DR form for the inverse, which reads

$$S^{-1} = \not{p} - m(\zeta) - \int ds \frac{[\not{p}\rho_v(s) + \rho_s(s)] \frac{p^2 - \zeta}{s - \zeta}}{p^2 - s + i\varepsilon}. \quad (115)$$

For this purpose we introduce the following convenient notation:

$$\begin{aligned} \hat{g} = \text{Re}S &= \frac{r}{\not{p} - m} + P. \int ds \frac{\hat{\sigma}(s)}{p^2 - s} \quad ; \quad \hat{\sigma}(s) = \not{p}\sigma_v(s) + \sigma_s(s), \\ \hat{d} = \text{Re}S^{-1} &= \not{p} - m(\zeta) - P. \int ds \frac{\hat{\rho}(s)}{p^2 - s} \frac{p^2 - \zeta}{s - \zeta} \quad ; \quad \hat{\rho}(s) = \not{p}\rho_v(s) + \rho_s(s), \end{aligned} \quad (116)$$

which allows us to rewrite the identity (114) as

$$(\hat{g} - i\pi\hat{\sigma}(p^2))(\hat{d} + i\pi\hat{\rho}(p^2)) = 1, \quad (117)$$

where we have used the well known functional identity for distributions (59). Comparing the real and imaginary parts of (117) we arrive at two coupled equations:

$$\begin{aligned} \hat{g}\hat{d} &= 1 - \pi^2\hat{\sigma}(p^2)\pi\hat{\rho}(p^2), \\ \hat{\sigma}(p^2)\hat{d} &= \hat{g}\hat{\rho}(p^2). \end{aligned} \quad (118)$$

Still in the matrix formulation introduced in Eq. (116) we can write

$$\hat{\sigma}(p^2)(\hat{d}^2 + \pi^2\hat{\rho}^2(p^2)) = \hat{\rho}(p^2), \quad (119)$$

i.e. \hat{g} is eliminated. Owing to this fact the principal value integrations over the unknown $\hat{\sigma}$ are not presented from now on. The Eq. (119) represents matrix form of Unitary Equations. For the purpose of completeness we will write them down also in terms of $\sigma_{v,s}$ explicitly. To this end we define two scalar functions $c_v(p^2)$ and $c_s(p^2)$ such that

$$\hat{d}^2 + \pi^2\hat{\rho}^2(p^2) = \not{p}c_v + c_s, \quad (120)$$

which implies

$$c_s = p^2\mathcal{A}^2 + \mathcal{B} + \pi^2(p^2\rho_v^2 + \rho_s^2) \quad ; \quad c_v = -2\mathcal{A}\mathcal{B} + 2\pi^2\rho_v\rho_s, \quad (121)$$

where we used shorthand notation for the real parts of the functions A, B

$$\begin{aligned} \mathcal{A} &= \text{Re}A(p^2) = 1 - P. \int ds \frac{\hat{\rho}_v(s)}{p^2 - s} \frac{p^2 - \zeta}{s - \zeta}, \\ \mathcal{B} &= \text{Re}B(p^2) = m(\zeta) + P. \int ds \frac{\hat{\rho}_s(s)}{p^2 - s} \frac{p^2 - \zeta}{s - \zeta}. \end{aligned} \quad (122)$$

Then “projecting” Eq. (119) by Tr and $Tr \not{p}$ we get, after a little algebra, the desired Unitary Equations:

$$\sigma_v = \frac{p^2 c_v \rho_v - c_s \rho_s}{p^2 c_v^2 - c_s^2} \quad ; \quad \sigma_s = \frac{c_v \rho_s - c_s \rho_v}{p^2 c_v^2 - c_s^2} \quad , \quad (123)$$

which are nonzero above the threshold, i.e. for $p^2 > m^2$. As in the previously discussed scalar model, the form of the Unitary Equations (123) does not depend on the details of interaction but on an analytical assumption – a spectral representation for the fermion propagator. Clearly, the Unitary Equations are formally equivalent to the Unitary Equations presented in the Ref. [13], but here with the main difference that all principal value integrals to be solved numerically are eliminated from now on. In our approximations the function $\mathcal{A} = 1$ and the real part of the mass function above the threshold is

$$\begin{aligned} \mathcal{B}(p^2) &= m(\zeta) + \frac{3\alpha_{QED}}{4\pi} \left\{ r m \left[1 - \left(1 - \frac{m^2}{p^2} \right) \ln \left(\frac{p^2}{m^2} - 1 \right) \right] \right. \\ &\quad \left. + \int_{m^2}^{\infty} d\alpha \sigma_s(\alpha) \left[1 - \left(1 - \frac{\alpha}{p^2} \right) \ln \left| \frac{p^2}{\alpha} - 1 \right| \right] \right\} . \end{aligned} \quad (124)$$

As we mentioned, the threshold singularity need not be real valued and the conventional procedure of extracting a real number r by on-shell differentiation of the self-energy function is inconsistent. However, the solution of this puzzle is very simple, recall here that the fixed renormalization uniquely determine the whole propagator function and thus the real pole part residuum r in (108) as well. Putting for instance $p = 0$ in (114) we get particularly simple formula for the residuum r

$$r = \frac{m}{m(\zeta) + \int_{m^2}^{\infty} \frac{\rho_s(x)\zeta}{x(x-\zeta)} dx} - \int_{m^2}^{\infty} \frac{\sigma_s(x)m}{x} dx . \quad (125)$$

The physical electron mass is defined by Eq. $\text{Re}S^{-1}(m) = 0$ or equivalently $M(m) = m$. Using the DRs (110),(111) the desired relation reads:

$$m = m(\zeta) + \int_{m^2}^{\infty} ds \frac{(m\rho_v(s) + \rho_s(s))(m^2 - \zeta)}{(m^2 - s)(s - \zeta)} . \quad (126)$$

However, here $\rho_{v,s}(m^2) = 0$ is necessary in order to have the correct definition of the physical mass. (This statement is clearly fulfilled in perturbation theory, see the first term in Eqs. (112),(124) for this purpose.)

The Unitary Equations (112),(123) have been solved by the method of iterations. The residuum (125), physical mass (126) and the mass function (124) have been evaluated at each step of the iteration procedure and substituted in the Unitary Equations until convergence is achieved.

To compare with the Euclidean space SDEs solutions we use the same renormalization condition in the both approaches, i.e. $B(-100) = 10$. Having all the numerical solutions stable and making comparison between Euclidean and

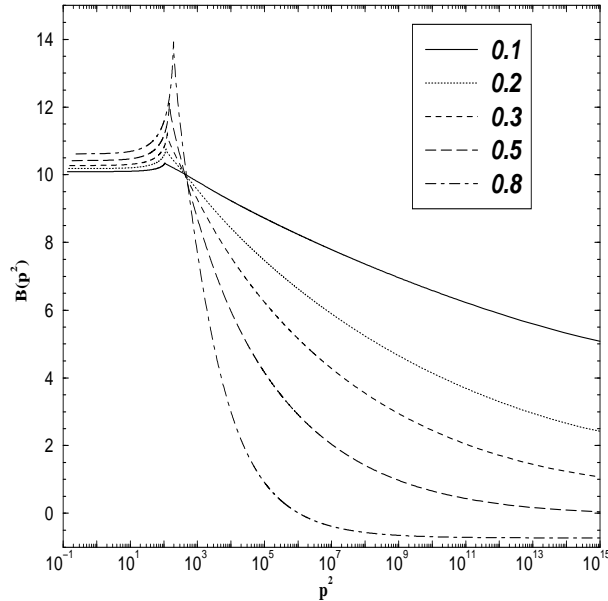


Figure 8. Timelike mass functions of the electron propagator as they have been obtained from solution of the Unitary Equations.

Minkowski results we have found that they perfectly agree when the coupling is small enough. The Unitary Equations resulting spacelike solutions for the mass function are compared in the Fig. 7. In Fig. 8 the Unitary Equations solutions are given for timelike momenta. The meaning of the origin of small numerical difference for strong couplings is not satisfactory understood. We can speculate here that the analytical spectral representation Ansatz does not fully capture the structure of the fermion propagator but we hope this point will be clarified in the future.

4.6 Approximate solution of dynamical chiral symmetry breaking in Minkowski space

In explicit chiral symmetry breaking case, in which the nonzero electron mass exists from the very beginning, both approaches— Minkowski and Euclidean— offer approximately the same results in the coupling constant domain where both solutions were obtained (in the spacelike momentum region, of course). These solutions were reviewed and compared in the previous Sections.

Until now, we have avoided the phenomenon of spontaneous chiral symmetry breaking which plays an important role in particle physics. The numerical methods used for rainbow Landau gauge approximation in the paper [13] enable to find a non-trivial solution of Unitary Equations for zero fermion Lagrangian mass. The numerical solution tended to fail near critical value $\alpha_c = \pi/3$ in rainbow approximation. In that case, approaching the coupling to its critical value the Unitary equations become less numerically stable. It was already observed that better stability can be achieved when nonzero mass is added into the gauge-boson propagator. The authors of the paper [75] were looking for the Minkowski

solution of the fermion SDE $\Sigma = \int KS$ with the effective kernel chosen as

$$\begin{aligned} K(q, p)_{ijkl} &= \gamma_{ij}^\alpha \gamma_{kl}^\beta \left[-g^{\alpha\beta} + \frac{q_\alpha q_\beta}{q^2} \right] G(q^2), \\ G(q^2) &= \frac{1}{q^2 - m_B^2 + i\epsilon} - \frac{1}{q^2 - m_A^2 + i\epsilon} \end{aligned} \quad (127)$$

In the case when $m_B \ll m_A$ the mass m_B can be understood as an infrared regulator while m_A represents ultraviolet (Pauli-Villars) one. For this simple model the gap equation has been solved in the Euclidean space and in Minkowski space as well. The nontrivial chiral symmetry breaking solutions have been compared for the first time. Within the spectral function Ansatz (108) the strategy of Unitary equations (123) has been used for the later purpose. In $A = 1$ approximation the explicit evaluation of finite selfenergy leads to the following result for the absorptive and dispersive part of the mass function

$$\begin{aligned} \rho_s(\omega) &= \frac{\alpha}{(4\pi)} \int dx \sigma_s(x) [X_0(\omega; m_B^2, x) - X_0(\omega; m_A^2, x)], \\ \mathcal{M}(p^2) &= \frac{3\alpha}{4\pi} \int dx \sigma_s(x) [J(p^2, x, m_B^2) - J(p^2, x, m_A^2)], \end{aligned} \quad (128)$$

where we have labeled

$$\begin{aligned} J(p^2, y, z) &= -\frac{\Theta(-\lambda_p)\sqrt{-\lambda_p}}{p^2} \left[\frac{\pi}{2} + \arctg \frac{p^2 - y - z}{\sqrt{-\lambda_p}} \right] + \frac{1}{2} \ln(16yz) \\ &- \frac{\Theta(\lambda_p)\sqrt{\lambda_p}}{p^2} \ln \left| \frac{p^2 - y - z + \frac{\lambda_p}{T - p^2}}{p^2 - y - z + \sqrt{\lambda_p}} \right| + \frac{\Theta(\lambda_0)\sqrt{\lambda_0}}{p^2} \ln \left| \frac{-y - z + \frac{\lambda_0}{T}}{-y - z + \sqrt{\lambda_0}} \right|, \end{aligned} \quad (129)$$

and the following abbreviations is introduced:

$$\begin{aligned} \lambda_p &= \lambda(p^2, y, z), \\ \sqrt{\lambda_0} &= |y - z|, \\ T &= (\sqrt{y} + \sqrt{z})^2. \end{aligned} \quad (130)$$

The function X is defined in (24).

These equations together with (123) comprise the coupled set of integral equation that have been solve numerically in [75]. Not strangely, the critical coupling $\alpha_c \sim \pi/3$ when $m_B \ll m_A$ which is expected from the study of rainbow QED with hard cutoff. More interestingly, the analytical continuation of (spectral) timelike solution to the spacelike regime is in rather good agreement with the Euclidean one, especially when the coupling is close enough to the critical value α_c . Furthermore, the trivial solution was found bellow α_c in both treatments. However, there is apparent deviation when the coupling increases. This, together with the authour's observation of the deviation from assumed analyticity implies that spectral solution is not the exact and true solution of original

SDE. It is suggested that deviation of 'Minkowski spectral' solutions from corresponding Euclidean ones reveals that the employed Ansatz, which fixes the analytical structure of propagator in Minkowski space, is not adequate for the case of the dynamical mass generation. It seems likely that with coupling increasing above its critical value, the pole of the propagator, located for subcritical case on the real axis, moves gradually into complex plane (i.e. receives non-negligible imaginary part) and the standard Lehmann representation, employed for our calculations, is not valid anymore.

However, checking the analyticity in the whole Minkowski space and also comparing spectral solution with the Euclidean ones at spacelike, one can conclude that the solution of Unitary Equations near the critical coupling is a rather good approximation. This approximative character become worse and worse when the coupling flows from its critical value, while the agreement is perfect at critical coupling (however were the result is trivial). At the end we can mention that within the Unitary Equations a given model neither provides the similar picture to the behaviour of light (say u,d,s) quark mass in QCD (here, the word 'similar' means the shape and slope of the mass function, or much simply the ratio of the value of mass function at two rather distinct scales). The analytical property of the solution in such a strong case remains unexplored at least by the presented method. For an different analytical guesses of the form of the quark propagator in modeled QCD see for instance [76].

4.7 Unquenched QED - calculation of the running coupling

In the previous Section we performed a numerical study of the electron mass function in the simple approximation to the SDEs: the bare vertex and photon propagators were employed. In what follows we extend these calculations: we solve the corresponding SDEs in Landau gauge also for the photon polarization function. We again compare the solutions for propagators in Minkowski and Euclidean space and we have found reasonable agreement between solutions obtained in these two technically rather different frameworks.

The 4D QED is trivial theory, in other words the presence of some regulator is required for any nonzero value of the renormalized coupling constant. It is convenient to introduce nonperturbative invariant continuum regulator function which also render finite the ultraviolet divergences. Such program, completed years ago, provides invariant regularization across all quantum field theories (for the review see the paper [77]). However in this paper we simply use spectral cutoff regulator Λ_S for the purpose of Minkowski calculation and the hard momentum cutoff Λ_H for the purpose of Euclidean calculation. Λ_H cuts the Euclidean momentum integrals while Λ_S represents the upper spectrum boundaries in GFs SR and DR. They have been put to be equal, $\Lambda_S = \Lambda_H$ assuming no significant affect on the results. By construction the Minkowski regulator does not violate translation invariance of the theory while Euclidean hard cutoff Λ_H do this. The same argument is also valid for the gauge invariance of the theory (assuming gauge invariant truncation of SDEs). The observed discrepancy between the Minkowski and the Euclidean solutions, although not so large, is the consequence of the regularization scheme dependence in the trivial theory.

There are many attempts [79, 80, 81, 82, 83, 84, 85] to estimate the form and its effect of the transverse part Γ_T of the full vertex $\Gamma = \Gamma_{BC} + \Gamma_T$ on the behaviour of fermion propagator. The eight independent component of Γ_T is the only unknown part of the fermion and photon SDEs system when solely written. The longitudinal part, named Ball-Chiu vertex Γ_{BC} is the minimal Ansatz consistent with Ward-Takahashi identity (91) (and of course with perturbation theory [78]). To derive dispersion relation for fermion selfenergy and photon vacuum polarization is complicated task even when Γ_{BC} is only considered (see [35]), therefore, instead of making some complicated Ansatz for the gauge vertex we consider the skeleton expansions of the Green functions. The skeleton expansion can be obtained from the sophisticated iteration of truncated SDEs system corresponding thus with approximated effective action. This so called Φ derivable approximation (or N-PI) of effective action is used in many branches of quantum field theory [86, 87, 88, 89, 90, 91, 92, 93, 94]. For an intimate relation between N-PI effective action and the full SDEs see the discussion in [95]. It is a systematically improvable method where the improvement is achieved by considering further and further terms in the loop expansion of the effective action. In the skeleton expansion there are only the classical vertices included in each skeleton diagram which make the calculation of DR more tractable. For a first attempt made in this paper we calculated the one loop skeleton contribution, the resulting gap equation corresponds with the SDEs in the bare vertex approximation. The study of SDEs where self-energies are considered in two loop skeleton expansion is now under consideration.

Further in order to reduce the complicated hierarchy of equations we explicitly put $A = 1$. Within several percentage deviation such approximation can be justified in Landau gauge herein [96, 45, 97].

4.8 Unquenched QED in Euclidean space

The SDEs are solved in Euclidean space after the Wick rotation $k_0 \rightarrow ik_{1E}$ is performed. Then the loop integrals should be free of kinematic singularities and the GFs are found for positive Euclidean momentum $k_E^2 = k_1^2 + k_2^2 + k_3^2 + k_4^2$.

Since we use the hard cutoff Λ_H in our Euclidean treatment the unpleasant quadratic divergence in the polarization function Π is generated in this case. Due to this we follow usual strategy [7, 96, 97] and avoid the quadratic divergence by the use of Bloch-Pennington projector

$$\begin{aligned} \mathcal{P}_{\mu\nu}^{(d)}(q) &= \frac{1}{d} \left[g_{\mu\nu} - (d+1) \frac{q_\mu q_\nu}{q^2} \right], \\ \Pi_E(q^2) &\equiv \frac{\Pi^{\alpha\beta}(q) \mathcal{P}_{\alpha\beta}^{(3)}(q)}{3q^2}. \end{aligned} \quad (131)$$

Employing this projection in the SDE for the photon propagator we arrive at the following coupled equations:

$$\Pi_E(x) = \frac{2\alpha}{3x\pi^2} \int dy \frac{y}{y + M_E^2(y)} \int d\theta \sin^2 \theta \frac{2y - 8y \cos^2 \theta + 6\sqrt{yx} \cos \theta}{z + M_E^2(z)},$$

$$(132)$$

$$M_E(x) = m_0 + \frac{\alpha}{2\pi^2} \int dy \frac{y}{y + M_E^2(y)} \int d\theta \sin^2 \theta \frac{3M_E(y)}{z(1 - \Pi_E(z))} , \quad (133)$$

where the variables x, y represent squares of Euclidean momenta, $z = x + y - 2\sqrt{yx} \cos \theta$.

After the subtraction

$$\begin{aligned} \Pi_E^R(\zeta'; p^2) &= \Pi_E(p^2) - \Pi_E(\zeta'), \\ M_E^R(\zeta'; p^2) &= M_E(p^2) - M_E(\zeta'). \end{aligned} \quad (134)$$

at some arbitrary ζ' and after renormalization, the Eqs. (132),(133) have been solved numerically. If needed the change of the renormalization scale choice is performed simply by the utilization of the identity

$$\Pi_E^R(\zeta; p^2) = \Pi_E^R(\zeta'; p^2) - \Pi_E^R(\zeta'; \zeta). \quad (135)$$

4.9 Unquenched QED in Minkowski space

Likewise in the ladder approximation of QED the SDEs written in momentum space are converted to the coupled set of Unitary Equations. The Unitary Equations (123),(125),(126) for fermion spectral functions is already derived in the previous Section. They remain unchanged since they follow from general analytic structure of the fermion propagator function. The Unitary Equation for the photon spectral function is derived bellow. Before doing this we review the DR for the fermion selfenergy in the presence of dressed photon propagator.

In $A = 1$ approximation we can identify the electron mass function (98) as

$$\begin{aligned} M(p^2) &= m_o + \frac{Tr}{4} \Sigma(p) = m_o + \\ e^2 \frac{Tr}{4} \int da \int db \int \frac{d^4 l}{(2\pi)^4} \gamma^\nu \frac{(\not{p} - \not{l}) \bar{\sigma}_v(a) + \bar{\sigma}_s(a)}{(p-l)^2 - a} \gamma^\mu \frac{-g_{\mu\nu} + \frac{l_\mu l_\nu}{l^2}}{l^2 - b} \bar{\sigma}_\gamma(b) \end{aligned} \quad (136)$$

which after the renormalization (add zero of the form $m(\zeta) - m(\zeta)$ into the Eq. (136) and make the subtraction) leads to the DR

$$M(p^2) = \int_{m^2}^{\infty} d\omega \frac{p^2 - \zeta}{\omega - \zeta} \frac{\rho_s(\omega)}{p^2 - \omega + i\varepsilon} + m(\zeta), \quad (137)$$

$$\rho_s(\omega) = -3 \left(\frac{e}{4\pi} \right)^2 \int da db \bar{\sigma}_s(a) \bar{\sigma}_\gamma(b) \frac{\lambda^{1/2}(\omega, a, b)}{\omega} \Theta(\omega - (\sqrt{a} + \sqrt{b})^2) \quad (138)$$

where σ_γ is the photon spectral function defined by the SR for photon propagator, which in the Landau gauge reads

$$\begin{aligned} G^{\mu\nu}(q) &= \int_0^{\infty} db \frac{\bar{\sigma}_\gamma(b) \left(-g^{\mu\nu} + \frac{q^\mu q^\nu}{q^2} \right)}{q^2 - b + i\varepsilon}, \\ \bar{\sigma}_\gamma(b) &= r_\gamma \delta(b) + \sigma_\gamma(b). \end{aligned} \quad (139)$$

Since gauge invariance is correctly maintained the photon polarization function should possess at most logarithmically superficial divergence. Therefore only one subtraction is needed and the DR for renormalized polarization function then looks like

$$\begin{aligned}\Pi_R^{\mu\nu}(\zeta; q^2) &= (q^2 g^{\mu\nu} - q^\mu q^\nu) \Pi_R(\zeta; q^2), \\ \Pi_R(\zeta; q^2) &= \int_0^\infty d\omega \frac{\rho_\gamma(\omega)(q^2 - \zeta)}{(q^2 - \omega + i\varepsilon)(\omega - \zeta)},\end{aligned}\quad (140)$$

where we use (not necessarily) the same renormalization scale as in the case of electron propagator.

In order to arrive to the photon Unitary Equation, the real and imaginary part of the identity $G_{\alpha\beta}^{-1} G^{\beta\gamma} = \delta_{\alpha\gamma}$ is evaluated. This, after using the definition of photon propagator (94) and the SR assumption (139) leads to the following identity:

$$[1 - \Pi_R(\zeta; q^2)] \left[\frac{r_\gamma}{q^2} + \int \frac{ds \sigma_\gamma(s)}{q^2 - s + i\varepsilon} \right] = 1. \quad (141)$$

For the next purpose we use shorthand notation for the function

$$b_\gamma(q^2) \equiv 1 - \text{Re} \Pi_R(\zeta; q^2) = 1 - P. \int_0^\infty ds \frac{\rho_\gamma(s)(q^2 - \zeta)}{(q^2 - s)(s - \zeta)}, \quad (142)$$

noting here that P. integration can be performed analytically at least at one (skeleton) loop level. Evaluating the real and the imaginary part of Eq. (141) gives

$$b_\gamma(q^2) \left[r_\gamma + P. \int ds \frac{\sigma_\gamma(s)}{q^2 - s} \right] = 1 - \pi^2 q^2 \rho_\gamma(q^2) \sigma_\gamma(q^2). \quad (143)$$

$$q^2 b_\gamma(q^2) \sigma_\gamma(q^2) - \rho_\gamma(q^2) \left[r_\gamma + q^2 P. \int ds \frac{\sigma_\gamma(s)}{q^2 - s} \right] = 0, \quad (144)$$

Putting together it yields resulting *Unitary Equation* for the photon spectral function:

$$\sigma_\gamma(q^2) = \frac{\rho_\gamma(q^2)}{q^2 [b_\gamma^2(q^2) + \pi^2 \rho_\gamma^2(q^2)]}. \quad (145)$$

where the functions σ_γ and ρ_γ are zero under the threshold $q^2 = 4m^2$.

The residuum r_γ of the photon propagator can be calculated from

$$r_\gamma = \frac{1}{1 - \Pi_R(\zeta; 0)}. \quad (146)$$

In the next text we will sketch the derivation of DR (140). First we briefly review the method in its perturbative context.

In $4 + \epsilon$ dimensions and for spacelike momentum $q^2 < 0$ the one loop polarization function can be written as [98]

$$\Pi(q^2) = \frac{4e^2}{3(4\pi)^2} \left\{ \frac{2}{\epsilon} + \gamma_E - \ln(4\pi) + \ln \left(\frac{m^2}{\mu_{t'H}^2} \right) - \frac{4m^2}{q^2} - \frac{5}{3} \right\}$$

$$+ (1 + 2m^2/q^2) \sqrt{1 - \frac{4m^2}{q^2}} \ln \left[\frac{1 + \sqrt{1 - \frac{4m^2}{q^2}}}{1 - \sqrt{1 - \frac{4m^2}{q^2}}} \right] \Big\} - \delta Z_3 \mu_{t'H}^{-\epsilon} , \quad (147)$$

where $\mu_{t'H}$ is t'Hooft scale. The mass-shell subtraction scheme defines Z_3 so that $\Pi_R(0; 0) = 0$ which implies that the photon propagator behaves as free one near $q^2 = 0$. Choosing δZ_3 to cancel entire $O(e^2)$ correction we find

$$\delta Z_3^{MASS} = \lim_{q^2 \rightarrow 0} \Pi(q^2) = \frac{e^2}{12\pi^2} \left[\frac{2}{\epsilon} + \gamma_E - \ln(4\pi) + \ln \left(\frac{m^2}{\mu_{t'H}^2} \right) \right] \quad (148)$$

and renormalized polarization function in mass-shell renormalization prescription satisfies well known DR:

$$\Pi_R(0; q^2) = \Pi(q^2) - \lim_{q^2 \rightarrow 0} \Pi(q^2) = \int_0^\infty d\omega \frac{q^2}{(q^2 - \omega + i\varepsilon)\omega} \rho(\omega) \quad (149)$$

where the absorptive part reads:

$$\pi\rho(\omega) = \frac{\alpha_{QED}}{3} (1 + 2m^2/\omega) \sqrt{1 - 4m^2/\omega} \Theta(\omega - 4m^2). \quad (150)$$

Recall that the one loop $\Pi_R(0, q^2)$ represents also self-energy calculated in the popular \overline{MS} scheme for the special choice of t'Hooft scale $\mu_{t'H} = m$. Clearly in off-shell momentum subtraction renormalization scheme: $\delta Z_3 = \Pi(\zeta)$ and the DR (149) is generalized to (140).

In our approximation the fermion propagator entering the photon SDE is dressed. Substituting SR for fermion propagator S into the photon polarization (88)

$$\Pi^{\mu\nu}(q) = ie^2 \int \frac{d^4 l}{(2\pi)^4} Tr [\gamma^\nu S(l) \gamma^\mu S(l - q)] , \quad (151)$$

and performing the standard steps we can arrive at DR where the weight function is now:

$$\begin{aligned} \rho_\gamma(q^2) &= \frac{e^2}{12\pi^2} \int da db \frac{\lambda^{1/2}(q^2, a, b)}{q^2} \left[1 + \frac{a+b}{q^2} - \frac{b-a}{q^2} \left(1 + \frac{b-a}{q^2} \right) \right] \\ &\quad \bar{\sigma}_v(a) \bar{\sigma}_v(b) \Theta \left(q^2 - (\sqrt{a} + \sqrt{b})^2 \right) . \end{aligned} \quad (152)$$

Clearly from the expression (152) follows that the functions $\rho_\gamma, \sigma_\gamma$ are nonzero only for $q^2 > 4m^2$.

4.10 Numerical comparison

Like in the ladder approximation considered previously the resulting set of Unitary Equations have been solved by numerical iterations. The cutoffs $\Lambda_S^2 = \Lambda_H^2 = 10^7 M^2(0)$ have been used and the renormalized mass is chosen such that $M(0) = 1$.

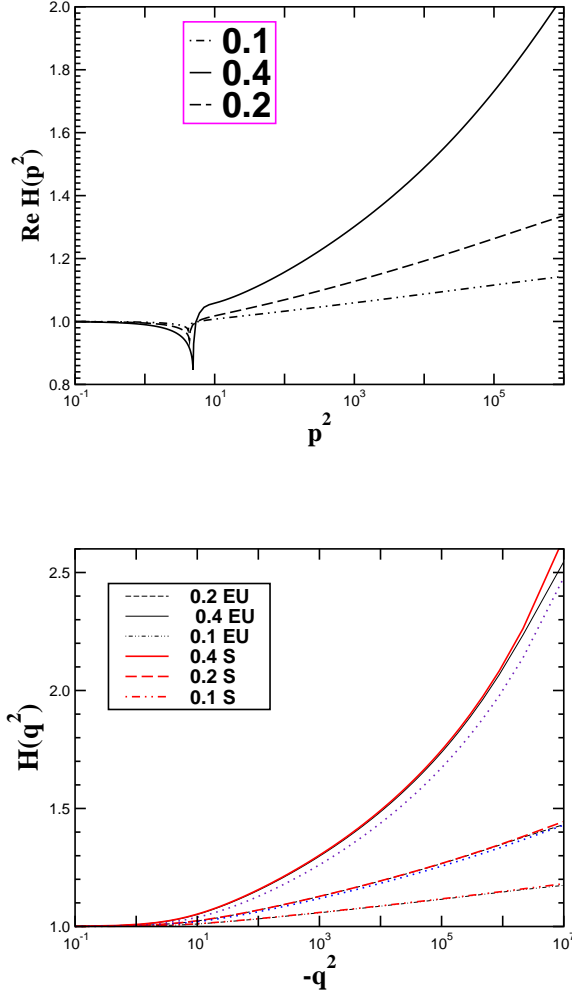


Figure 9. a) Top figure shows charge renormalization function $H = (1 - \Pi_R)^{-1}$ for timelike momenta for the renormalized couplings: $\alpha(0) = 0.1, 0.2, 0.4$. The down oriented peak corresponds to the threshold $4m^2$. b) Bottom figure displays charge renormalization functions for spacelike momenta as obtained by the solution of the SDEs in Euclidean (EU) and Minkowski (S) space are shown in the right figure. Dotted lines stand for one loop perturbation theory.

The solutions for the running couplings for timelike momenta as have been obtained from the Unitary Equations are displayed in Fig. 9. For better visualization the so called photon renormalization function $H_R = [1 - \Pi_R(\zeta; q^2)]^{-1}$ is actually plotted. The spectral and Euclidean solutions are compared in Fig. 9 too. Fermion mass function obtained from SDEs is displayed for spacelike regime of momenta in Fig. 10. The observed deviation of Euclidean results from the spectral ones can be explained as a consequence of different cutoffs concepts used in the Euclidean and Minkowski treatment. The timelike solution for M is shown in Fig. 10a) where the absorptive part is also added. We compare, too, with one loop perturbation theory. In this case we use the pole mass obtained from

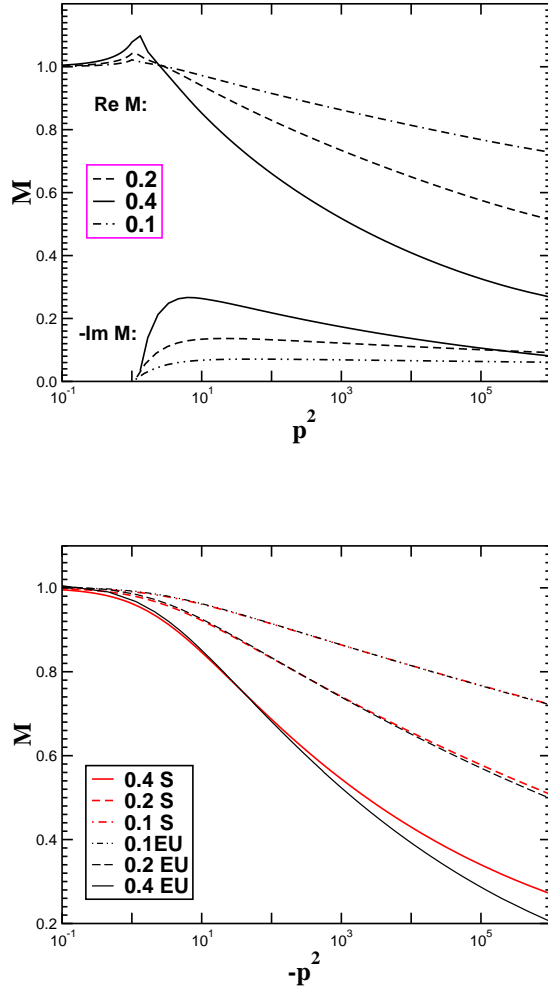


Figure 10. a) Upper panel displays the mass function $M(p^2)$ for timelike momenta. Note, the sign of the imaginary part, i.e. of $(\pi\rho_s(p^2))$. b) The lower panel displays comparison of mass function $M(p^2)$ calculated in Euclidean (EU) and in Minkowski (S) formalism for spacelike momenta now.

Unitary Equations as an input for one loop on-shell renormalized perturbation theory expression.

The large growth of the running coupling with its derivative close to the cutoff (see Fig. 9) signals a good evidence for the Landau singularity [99] and hence QED triviality. As the consequence of QED triviality the collapse of the both Spectral and Euclidean solution is observed. Contrary to quenched approximation, using the spectral approach here, we have always identified the physical pole mass which is probably the consequence of the smallness of the coupling at low q^2 .

$$\Pi^{\mu\nu}(q) = \text{[Diagram 1]} + \text{[Diagram 2]} + \text{[Diagram 3]} + \text{[Diagram 4]} + \text{[Diagram 5]} + \text{[Diagram 6]}$$

Figure 11. Diagrammatical representation of the Schwinger-Dyson equation for gluon self-energy. All internal propagators are dressed, as well as the vertices labeled by blobs. Wavy lines represent gluons, dashed lines represent ghosts and the solid lines stand for quarks.

5 Summary on the Unitary Equations

6 Analyticity of Green's functions in QCD

6.1 Motivation

Quantum Chromodynamics (QCD) is the only experimentally studied strongly interacting relativistic quantum field theory. This non-Abelian gauge theory with a gauge group $SU(3)$ has many interesting properties. The dynamical breaking of chiral symmetry explains why the pions are light, identifying them with the pseudo-Goldstone bosons associated with the symmetry breaking of the group $SU(2)_L \times SU(2)_R$ to $SU(2)_V$ (in flavor space). Asymptotic freedom [105, 106] implies that the coupling constant of the strong interaction decreases in the ultraviolet region. For less than $33/2$ quark flavors, QCD at high energy becomes predictable by the perturbation theory. However, in the infrared region the perturbation theory does not work and nonperturbative techniques have to be applied.

One of the most straightforward nonperturbative approaches is a solution of the SDEs for QCD. The extensive studies were undertaken for a quark SDE, based on various model assumptions for a gluon propagator. These approximate solutions, often accompanied by a solution of the fermion-antifermion Bethe-Salpeter equation for meson states, have become an efficient tool for studies of many nonperturbative problems, e.g., the chiral symmetry breaking, low energy electroweak hadron form factors, strong form factors of exclusive processes, etc. (see reviews [4, 5, 6, 107, 108] and also recent papers [7, 109, 110, 111, 112]).

However, to take gluons into account consistently is much more difficult than to solve the quark SDE alone. The SDE for the gluon propagator (see Fig. 11) is more nonlinear than the quark one. Moreover, the Fadeev-Popov ghosts have to be included [113] in a class of Lorentz gauges. In a class of covariant linear

gauges the contributions to the gluonic polarization function are sketched in Fig. 11. Although it is not so difficult to derive and write down the formal dispersion relation for vacuum polarization function (especially when one use bare vertices) we were not yet able to succeed with a numerical solution of Unitary Equations. Therefore, after a brief overview of selected representative SDEs solutions in Yang-Mills theory, instead of solving the SDEs we use the generalized (nonpositive) spectral representation to fit the spectral function to Euclidean solutions obtained in recent lattice simulations. This is a first step towards the understanding of analytical structure of infrared QCD.

6.2 Cornwall's approach

In this section we mention a symmetry preserving gauge invariant solution to gluon propagator obtained by Cornwall two decades ago [61]. To our knowledge this is the best published example, in which the behavior of the QCD Green function in the whole range of Minkowski formalism is addressed within the framework of the SDEs and spectral technique. To this end, the gauge invariant GFs have been constructed by means of the Pinch Technique. To achieve this particular spectral Ansatz for GFs were employed. The resulting vacuum polarization function is then by construction gauge-fixing independent. We leave aside the consistent nonperturbative proof of this statement, but we refer to the appropriate perturbative proof in ref. [56]. Let us now describe the basic steps of Cornwall's procedure.

As in the usual approach, the gauge fixing is imposed in the first step: The light-cone axial gauge is employed. Avoiding thus SR for ghosts, only the following SR for the gluon propagator is assumed:

$$G_{\mu\nu}(q) = P_{\mu\nu} G(q^2) = P_{\mu\nu} \int d\omega \frac{\sigma(\omega)}{q^2 - \omega + i\epsilon}, \quad (153)$$

$$P_{\mu\nu} = -g_{\mu\nu} + \frac{n_\mu q_\nu + n_\nu q_\mu}{(n \cdot q)}, \quad (154)$$

where for n_μ it holds $n_\mu n^\mu = 0, n \cdot A = 0$. $G(q^2)$ is the gauge-fixing independent scalar part of the gauge-invariant propagator $G_{\mu\nu}(q)$. The Ward identity

$$k_1^\alpha \Gamma_{\alpha\beta\gamma}(k_1, k_2, k_3) = G_{\beta\gamma}^{-1}(k_2) - G_{\beta\gamma}^{-1}(k_3). \quad (155)$$

between the gluon propagator and the three-gluon vertex $\Gamma_{\alpha\beta\gamma}(k_1, k_2, k_3)$ has to be satisfied. To enforce this identity the Gauge Technique was used, which makes the following Ansatz for the longitudinal part of the untruncated three-gluon proper GF:

$$\begin{aligned} G_{\alpha\beta\gamma} &= G^{\beta\beta'}(k_2) \Gamma_{\alpha\beta'\gamma'}^L G^{\gamma\gamma'}(k_3) \\ &= \int d\omega \bar{\sigma}(\omega) \left[\frac{P^{\beta\beta'}(k_2)}{k_2^2 - \omega + i\epsilon} \Gamma_{\alpha\beta'\gamma'}^{(\omega)}(k_1, k_2, k_3) \frac{P^{\gamma\gamma'}(k_3)}{k_3^2 - \omega + i\epsilon} \right]. \quad (156) \end{aligned}$$

Recall that the Gauge Technique was originally developed by Salam [114] as an attempt to solve a vector electrodynamics and later extended and applied to the scalar [64] and fermion [115] QED, for later studies based on the

Gauge Technique see [116, 117, 118, 119]. Substituting the Ansatz (156) into the approximate pinched gluon SDE [61] yields for the inverse of $G(q^2)$:

$$\begin{aligned} G^{-1}(q^2) &= q^2 - \Pi(q^2) \\ &= Z_3 \left\{ q^2 \left[1 + \frac{ibg^2}{\pi^2} \int d^4k \int d\omega \frac{\sigma(\omega)}{[(k+q)^2 - \omega](k^2 - \omega)} \right] \right. \\ &\quad \left. + \frac{ibg^2}{11\pi^2} \int d^4k \int d\omega \frac{\omega\sigma(\omega)}{[(k+q)^2 - \omega](k^2 - \omega)}, \right. \end{aligned} \quad (157)$$

$$\left. - \frac{i4bg^2}{11\pi^2} \int d^4k G(k^2) \right\}, \quad (158)$$

where b is the lowest-order coefficient in the β function

$$\beta = -bg^3 + \dots, \quad b = \frac{33}{48\pi^2}, \quad (159)$$

and Z_3 is the coupling renormalization constant:

$$Z_3 = g^2/g_0^2. \quad (160)$$

Equation (157) was not solved directly in Minkowski space, it was converted into the Euclidean space. Defining

$$d(q^2) = -G(-q^2), \quad (161)$$

it was found that the trial propagator

$$\begin{aligned} d^{-1}(q^2) &= [q^2 + m^2(q^2)] b g^2 \ln \left[\frac{q^2 + 4m^2(q^2)}{\Lambda^2} \right], \\ m^2(q^2) &= m^2 \left[\frac{\ln \left(\frac{q^2 + 4m^2}{\Lambda^2} \right)}{\ln \frac{4m^2}{\Lambda^2}} \right]^{-12/11}, \end{aligned} \quad (162)$$

where g, m and Λ are fitted parameters, is an excellent fit to the numerical solution of Eq. (157). The scale is fixed by the condition $d^{-1}(q^2 = \zeta) = \zeta$, where ζ is the renormalization scale [61].

Let us stress the main physical results obtained from the combination of the spectral Gauge and Pinch techniques. First of all it seems possible to reorganize the SDEs of QCD into a form which allows to deal directly with a gauge independent GFs. The second important feature is that the solution has a mass gap. There is no singularity corresponding with massless excitation since the gluon propagator is finite at zero momenta. For low q^2 the mass $m(q^2)$ varies within 500 ± 200 MeV, for large q^2 it vanishes, in agreement with the expected (perturbative) UV behavior. Note that similar behavior was obtained by the operator product expansion method several years later in [120]:

$$m^2(Q^2) \simeq \frac{34N_c}{\pi^2 9(N_c^2 - 1)} \frac{\langle \frac{\alpha_s}{\pi} F_{\mu\nu} F^{\mu\nu} \rangle}{Q^2}, \quad (163)$$

where Q is the gluon Euclidean momentum, $\langle \frac{\alpha_s}{\pi} F_{\mu\nu} F^{\mu\nu} \rangle$ is the gluon condensate [121] and $N_c = 3$.

Let us recall also some recent results supporting the idea (suggested long time ago [122]) of the dynamical gluon mass. It should be emphasized that the gluon “mass” is not a directly measurable quantity, but it can be related to other physical quantities. The lattice results [123, 124, 125, 126, 127, 10] seem to support this concept. Parisi and Petronzio [122] were first to introduce it into description of J/ψ decays.

6.3 Gluons and ghost in linear covariant gauges

The solution of SDEs in strong coupling non-Abelian theory like infrared QCD is strongly dependent on the gauge fixing of the QCD action and on the truncation of equations system as well. Since the coupling increases as one goes from the ultraviolet to the lower square of momenta, various approximations can lead to the different analytical properties of Green’s functions. A quite selfcontaining history of SDEs approach and phenomenology in QCD can be find in the paper [128] where the present knowledge about the infrared behaviour of QCD Green’s functions is summarized in the review (see eg. the Chapter 5). Here we will briefly mention the main results obtained in the Landau gauge, noting that the most of the recent results are obtained in this gauge.

In the initial study of SDEs [129] Mandelstam provisionally neglected the effect of ghosts. As the consequence of this first approximation it was shown that gluon propagator is more singular then simple pole in this case. Using the similar truncation this behaviour was confirmed in the studies [130, 131]. It was first suggested in [132] that such behaviour is not an inherent property of nonperturbative dynamics of Landau gauged QCD but rather of deficiency of truncation of SDEs system. It was suggested that this is not gluon, but rather ghost propagator that is highly singular in the zero momentum limit. The detailed analytical and numerical study of the coupled ghost and gluon equations in Landau gauge with bare vertices was made [133, 134]. It was actually confirmed that the ghost loop dominates the infrared behaviour of the gluon propagator. In recent papers [7, 9, 136, 137, 138] studies of the coupled SDEs for gluon and ghost propagators in the usual Landau gauge in Euclidean space were performed in various approximations. An interesting result of the investigations in Landau gauge is the observation, that there is no qualitative difference of the solutions found with bare vertices or with vertices dressed by the use of Slavnov-Taylor identities. Note that the similar behaviour was observed in the wide class of ghost-antighost symmetric gauges [139]. The attempt to estimate the effect of two loop irreducible contributions was made in [9]. The numerical result indicates slight changes in the intermediate regime. Note that the inclination of this result towards the lattice data was shown already in the introduction of presented paper.

6.4 Analytical continuation of Euclidean solutions

The assumption of GF’s analyticity and hence the assumption of the propagator spectral representation was key point for the formulation of the Unitary

Equations and the solution of SDEs in Minkowski space. The requirement of the propagator (or invariant charge) analyticity is supposed to be a good assumption in QCD for many reasons [140, 141, 142, 104] and the analytical structure of the GFs obtained from Euclidean SDEs in QCD is under current investigation [76].

In this Section we perform analytical continuation of recent unquenched lattice results [1] for gluon propagator to the Minkowski space. Note that the similar fit has been already performed for the case of pure gluodynamics [35] where the quenched lattice data [10] has been used. In the paper [1] the authors considered three flavor QCD. For this purpose one massless and one massive quark have been taken into account. The main difference that follows from unquenching of lattice gluon propagator is the partial suppression of infrared enhancement plateau. For some details see the original paper [1] where the comparison is made. Of course, taking the effects of quark-antiquark pairs into account it has no influence on the main characteristic feature of the Landau gauge gluon propagator: it is obviously infrared vanishing function. Therefore, in contrast to the propagator of a stable unconfined particle, we assume that the spectral function is a smooth real function, i.e., propagator has not simple pole structure.

In fact, what we actually do, it is the continuation of the data obtained for a real negative momentum semiaxis to the border of analyticity domain. This is the standard situation when one makes prediction from experimentally obtained data to the experimentally inaccessible regime (the extraction of nucleon spectral function from the electromagnetic form factor is a good example). This approach has been already extended to the case of gluon spectral function of $SU(2)$ Yang-Mills theory ref. [143]. However, in our case, the smallness of errors of the lattice simulations and the value of lattice spacing as well allows to use the data directly for our purpose. No extrapolation to higher square of momenta is made and we neglect the computational errors as well.

The gluon spectral function $\sigma(\omega)$ and the most probable analytical fit is obtained from the minimization of

$$I_{fit} = \sum_i \left[\tilde{H}(x_i) - H(x_i) \right]^2, \quad (164)$$

$$(165)$$

where H is the gluon form factor defined as $H(x) = xG(x)$, $\tilde{H}(x)$ are the appropriate lattice data evaluated for the square of momenta $x = q_E^2$ while $H(x)$ is obtained through the fit of the spectral function which enters the generic SR for the gluon propagator in the Landau gauge which reads

$$G_{AB}^{\alpha,\beta}(q) = \delta_{AB} \left[-g^{\alpha\beta} + \frac{q^\alpha q^\beta}{q^2} \right] G(q^2),$$

$$G(q^2) = \int_0^\infty d\omega \frac{\sigma(\omega)}{q^2 - \omega + i\epsilon}, \quad (166)$$

where A, B are color indices. The Ansatz (166) should be considered as the generalized spectral representation, since we do not assume (and do not obtain) the spectral function $\sigma(\omega)$ positive for all values of ω . For completeness let us note

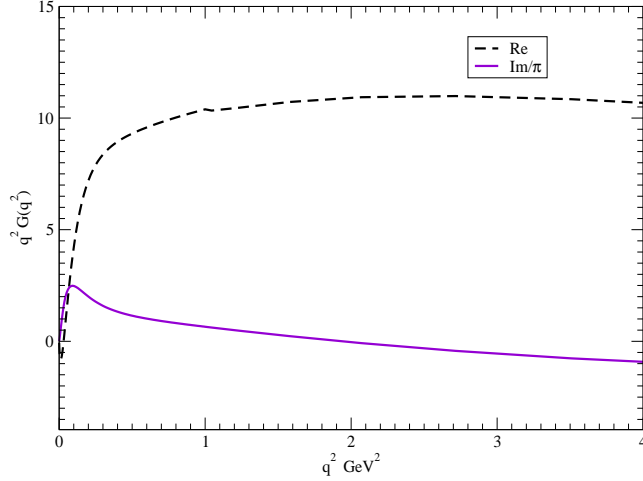


Figure 12. The extrapolated gluon form factor $H(x) = xG(x)$ at timelike momentum axis.

that we use unrenormalized data, i.e. the suitable but for us irrelevant constant prefactor should be added when considered for some application.

To achieve a reasonable accuracy we use the following iterative minimizations procedure: The function H_J evaluated at some J -step of our iteration cycle is in each case obtained by the previously obtained fit for spectral function, i.e. σ_{J-1} such that the relation for H_J reads:

$$H_J(x_i) = x_i \int_0^\infty d\omega \frac{\sigma_{J-1}(\omega)}{x_i + \omega} \sum_{l=0}^3 a_l P_l(z), \quad z = \frac{\omega - c}{\omega + c}, \quad (167)$$

where a_i are dimensionless constant coefficients of Legendre polynomial which are fitted during the minimization procedure, c is positive massive parameter which is used for the fit as well. Some suitable zeroth iteration input is used for σ_0 . For this purpose we use the convenient choice of the form: $\sigma_0(\omega) = K \frac{\log^{-\gamma-1}(e+\omega/\Lambda^2)}{\omega+\Lambda^2}$ with some suitable parameters K, γ, Λ . Assuming that the procedure is convergent then the best fit is then obtained when $a_0 = 1$ and other coefficients of Legendre polynomial are zero, which should be true irrespective of the value of the constant c . We actually observe the relatively fast convergence of the described process and we stopped our minimization procedure when $a_0 = 1.0006$ and other a 's are at most few of 10^{-3} . Such minimization procedure is much more powerful than to perform minimization at once time with some 'more suitable' function even with larger number of the fitting parameters. As a bonus the computer time is reasonably short (seconds for office PC).

For a vanishing gluon propagator we have the following "sum rule" for σ

$$G(0) = \int_0^\infty \frac{\sigma(\omega)}{\omega} \simeq 0, \quad (168)$$

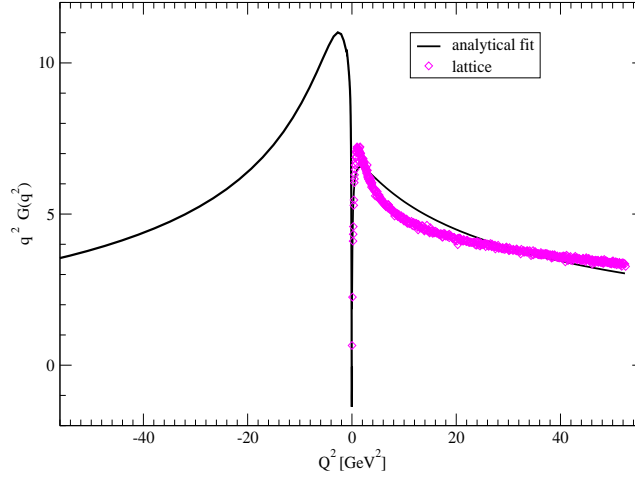


Figure 13. Gluon propagator for $N_f = 3$ QCD, the lattice data [1] are represented by diamonds. The fit (at spacelike) and the extrapolation (at timelike) is labeled by solid line.

which is clearly impossible for the positive σ . Note that the violation of positivity was confirmed by some other lattice simulations [144], where it was indicated by the study of Schwinger function. The extrapolated solution is plotted in Fig. 12. The spectral function has a positive peak at the infrared and becomes negative for asymptotically large p^2 . The infrared behaviour describes the shortlived gluon excitation and is consistent with the absence of gluon in the physical spectrum while the large momentum behaviour is the feature already expected from the perturbation theory. Clearly, the observed shape of the gluon propagator in Landau gauge is in accord with our physical expectations, e.g. with the confinement of color object and asymptotic freedom as well.

In Fig. 13 we also display our fit at the spacelike regime and provide the comparison with the original lattice data [1]. The real part of extrapolated gluon propagator is added for comparison too (negative Q^2 semiaxis now). From this we can see that we were not able to fit the lattice data exactly. The origin of this small discrepancy can be a combination of several effects: it can be artifact of our iteration/minimization procedure, it can signal the the complex singularities however positioned rather close the real positive momentum square semiaxis, partially it can be a consequence of finiteness of the lattice spacing and finite lattice volume. This complications could be clarified in future studies but they have a little significance for the main statement: The Landau gauge gluon propagator is the analytical function in the whole complex plane with the exception of (or small vicinity of) a real positive semiaxis of square of momenta and it can be parameterized (or at least reasonable approximated) by nonpositive spectral representation.

7 Summary, conclusion and outlook

An important question, in field theory in general, and in the SDE approach particular, is the connection between Euclidean-space and physical Minkowski space. As we explicitly demonstrated it is clear that to perform SDEs studies directly in Minkowski space is possible.

We began with an introduction to the analytical concept in the formalism of Schwinger-Dyson equations with specific emphasizes to the derivation and solution of the Unitary Equations in scalar models and QED. For the later case we presented studies of strong-coupling QED in different approximations. One of them was unquenched QED, which represents the study where the running of the coupling has been correctly taken into account. In this case the QED triviality plays its own crucial role in the asymptotically large spacelike momenta and we explain how to deal with this trivial theory correctly within the formalism of spectral representations and dispersion relations. The Unitary Equations presented are systematically improvable by considering further and further skeleton contributions to the effective action. If the analyticity is correctly maintained then the all momentum integrations can be performed analytically. For instance, let us consider the two-loop improved approximation of our scalar model considered in the Section 3. In this case it is sufficient to add the contribution from the two-loop graphs to the weight function (58), i.e.

$$\rho(p^2) \rightarrow \rho(p^2) + \rho_{sun}(p^2) + \dots, \quad (169)$$

where $\rho_{sun}(p^2)$ is given by rhs. of Eq.(33) and the dots stand for the terms stemming from the two other known skeletons not explicitly considered here. This is a clear technical advantage of the presented method: we can immediately apply the known original results for absorptive parts of Feynman diagrams when they were already evaluated in perturbation theory.

For an explicitly massive theory and up to the certain values of the coupling constant the accurate comparison of SDEs solutions at spacelike momentum axis with the solutions performed by more conventional strategy in Euclidean space gives us strong belief in the relevance of presented methods. In this cases the only limitation of spectral method is given by the increasing number of spectral integrals in the expression for DR that is directly dictated by the number of internal propagators. Nevertheless, within contemporary power of computer facilities many of exciting calculations can be made and remain to be done.

The strong coupling QED is often regarded as an reasonable pedagogical tool for SDE studies and their application to QCD. We also attempted to extend the discussion to QCD where the direct Minkowski space formulation and solution is presently prevented by the partial lack of information on the timelike axis. While many important steps have been accomplished, it is apparent that much more needs to be done. Furthermore, at present time and up to a few exeptions, the vast amount of studies dealing with the deep nonperturbative phenomena like chiral symmetry breaking and dynamical mas generation were carried out in Euclidean space. Regarding the real QCD, it is not clear when or if it will be possible to perform such symmetry breaking SDEs studies directly in Minkowski space.

Another interesting prospective is to further explore the timelike infrared behavior of Green's functions by analytical continuation of presented lattice studies. We offered the solution for Landau gauge gluon propagator, but the information about the timelike structure of quark propagator is currently unavailable. The present day great improvements in the QCD lattice studies could provide significant benefits at this area in the recent and in the near future.

We also collected the necessary information and illustrated how it can be used in relativistic bound state calculations using the spectral representation for solving the Bethe-Salpeter equation in (3+1) Minkowski space. To further develop the method, it would be interesting to extend it to more complicated kernel: trying to include the cross boxed contributions, s and u channel interactions etc. It is already known that the "spectral approach" used here is suitable even for more complicated systems. The same or very similar tricks and technology when successfully performed in the Minkowski calculation could become great goals in hadronic physics in the not too distant future. As it is already known the obstacles due to fermionic degrees of freedom can be overcome. The solution of the spinless bound state (pion) composed from two quarks interacting via dressed gluon exchange is under auspicious consideration.

Acknowledgments

I am grateful to Jiří Adam, jr. for the stimulating discussions and useful comments. The author thank to P. Bowmann for sending me the recent lattice data. The author also thank to W. Guttinger, M.B. Halpern and B. Mihaila for the useful correspondence. This work is supported in part by the grant GAČR 202/03/0210 and by the ASCR project K1048102.

Appendix A:

The standard trick is to re-write the integral $J(p^2)$ in terms of the Feynman parameterization:

$$\begin{aligned}
J(p^2) &= \int \frac{d^d k_1}{(2\pi)^d} \int \frac{d^d k_2}{(2\pi)^d} \int_0^1 dx \frac{D(k_2 + p, \alpha_3)}{[k_1^2 + k_2^2 x(1-x) - \alpha_1 x - \alpha_2(1-x) + i\varepsilon]^2} \\
&= \int \frac{d^d k_2}{(2\pi)^d} \int_0^1 dx \frac{i D(k_2 + p, \alpha_3) \Gamma(2-d/2)}{(4\pi)^{d/2} [x(1-x)]^{2-d/2} \left[k_2^2 - \frac{\alpha_1}{1-x} - \frac{\alpha_2}{x} + i\varepsilon \right]^{2-d/2}} \\
&= \int_0^1 dx dy \int \frac{d^d k_2}{(2\pi)^d} \frac{i(4\pi)^{-d/2} \Gamma(3-d/2) y^{1-d/2}}{[x(1-x)]^{2-d/2}} \\
&\quad \frac{1}{\left[k_2^2 + p^2 y(1-y) - \left[\frac{\alpha_1}{1-x} - \frac{\alpha_2}{x} \right] y - \alpha_3(1-y) + i\varepsilon \right]^{3-d/2}} \\
&= \int_0^1 dx dy \frac{(-)^{2-d/2} \Gamma(3-d) y^{1-d/2}}{(4\pi)^d [x(1-x)]^{2-d/2} [y(1-y)]^{3-d} (p^2 - \Omega + i\varepsilon)^{3-d}} \\
\Omega &= \frac{S(x)}{1-y} + \frac{\alpha_3}{y} \quad ; \quad S(x) = \frac{\alpha_1}{1-x} + \frac{\alpha_2}{x} .
\end{aligned} \tag{A.1}$$

To make the subtractions (28) it is convenient to use the following Feynman formula:

$$A^{-q} - B^{-q} = \int_0^1 dw \frac{q(B-A)}{[(A-B)w + B]^{q+1}} . \tag{A.2}$$

Using variable z for the mass subtraction and the variable u for the subtraction of the term with derivative, we can immediately write down a formula for renormalized J :

$$J_R(p^2) = J(p^2) - J(\zeta) - \left. \frac{dJ(p^2)}{dp^2} \right|_{p^2=\zeta} (p^2 - \zeta) = \int_0^1 \frac{dx dy dz du \Gamma(5-d) z(-1)^{2-d/2} y^{1-d/2} (p^2 - \zeta)^2}{(4\pi)^d [x(1-x)]^{2-d/2} [y(1-y)]^{3-d} [(p^2 - \zeta)zu + \zeta - \Omega + i\varepsilon]^{5-d}}. \quad (\text{A.3})$$

In four dimensional spacetime the integral (A.3) is already finite and the limit $d \rightarrow 4$ can be simply taken.

In addition we make the following substitution: $\omega = \zeta + \frac{\Omega - \zeta}{zu}$. After changing ordering of the integrations $d\omega \leftrightarrow dz$ and integrating over z gives:

$$J_R(p^2) = \int_0^1 dx dy \int_{\Omega}^{\infty} d\omega \frac{(p^2 - \zeta)^2 (\omega - \Omega)}{(4\pi)^4 (\omega - \zeta)^2 (p^2 - \omega + i\varepsilon)}. \quad (\text{A.4})$$

Notice that all x, y dependence is now hidden in the lower bound Ω , which is defined in last line of (A.1). It is still possible to evaluate one more integral analytically, we have chosen to take the integral over y . Changing again the order of integrations we get for boundaries:

$$\int_0^1 dy \int_{\Omega}^{\infty} d\omega \rightarrow \int_{(\sqrt{S(x)+\sqrt{\alpha_3}})^2}^{\infty} d\omega \int_{y_-}^{y_+} dy, \quad (\text{A.5})$$

where y_-, y_+ are the roots of the equation $\omega - \Omega = 0$:

$$y_{\pm} = \frac{\omega - s + \alpha_3 \pm \sqrt{\lambda(S(x), \omega, \alpha_3)}}{2\omega}, \quad (\text{A.6})$$

where $\lambda(x, y, z)$ is the triangle function defined in (24). After the explicit integration over y and changing order of the last two integrals we arrive at the following result:

$$J_R(p^2) = \int_{(\sqrt{\alpha_1+\sqrt{\alpha_2+\sqrt{\alpha_3}}})^2}^{\infty} d\omega \frac{(p^2 - \zeta)^2 \rho_J(\omega)}{(\omega - \zeta)^2 (p^2 - \omega + i\varepsilon)} \quad (\text{A.7})$$

$$\rho_J(\omega) = \frac{1}{(4\pi)^4} \int_{x_-}^{x_+} dx \left[\frac{(\omega - S(x) + \alpha_3) \sqrt{\lambda(S(x), \omega, \alpha_3)}}{\omega} - \alpha_3 \ln \left(\frac{\omega - S(x) + \alpha_3 + \sqrt{\lambda(S(x), \omega, \alpha_3)}}{\omega - S(x) + \alpha_3 - \sqrt{\lambda(S(x), \omega, \alpha_3)}} \right) \right], \quad (\text{A.8})$$

$$x_{\pm} = \frac{(\sqrt{\omega} - \sqrt{\alpha_3})^2 + \alpha_1 - \alpha_2 \pm \sqrt{\lambda(\alpha_2, \alpha_1, (\sqrt{\omega} - \sqrt{\alpha_3})^2)}}{2(\sqrt{\omega} - \sqrt{\alpha_3})^2}.$$

If the omitted prefactor is restored Eq. (A.7) we can simply identify the one dimensional integral representation for imaginary part of Π_R/π .

This result can be rewritten into the form already available in literature [24],[25]. To this end we have to make the following substitution $x \rightarrow s$ such that

$$\begin{aligned} s &= S(x) \quad ; \quad \implies \\ x &= \frac{s + \alpha_1 - \alpha_2 + \sqrt{\lambda(\alpha_2, \alpha_1, s)}}{2s} \quad \text{for } x > x(s = (\sqrt{\alpha_1} + \sqrt{\alpha_2})^2) \\ x &= \frac{s + \alpha_1 - \alpha_2 - \sqrt{\lambda(\alpha_2, \alpha_1, s)}}{2s} \quad \text{for } x < x(s = (\sqrt{\alpha_1} + \sqrt{\alpha_2})^2) \end{aligned} \quad (\text{A.9})$$

which leads to the relation given in [24],[25]:

$$\rho_J(\omega) = \frac{1}{(4\pi)^4} \int_{(\sqrt{\alpha_1+\sqrt{\alpha_2}})^2}^{(\sqrt{\omega}-\sqrt{\alpha_3})^2} ds \frac{\sqrt{\lambda(s, \omega, \alpha_3)} \sqrt{\lambda(\alpha_2, s, \alpha_1)}}{s\omega} \Theta \left(\omega - \left(\sum_{i=1}^3 \alpha_i^{1/2} \right)^2 \right). \quad (\text{A.10})$$

References

1. P.O. Bowman, U.M. Heller, D.B. Leinweber, M.B. Parappilly, A.G. Williams, Phys.Rev. **D70**, 034509 (2004).
2. P.O. Bowman, U.M. Heller, D.B. Leinweber, M.B. Parappilly, A.G. Williams, Phys.Rev. **D70**,034509 (2004).
3. P.O. Bowman, U.M. Heller, D.B. Leinweber, M.B. Parappilly, A.G. Williams, Jianbo Zhang, Phys.Rev. **D71**, 054507 (2005)
4. C.D. Roberts, A.G. Williams, Prog. Part. Nuc. Phys. **33** (Pergamon Press, Oxford,) 1994.
5. R. Alkofer, L. von Smekal, Phys. Rep. **353**, 281 (2001).
6. P. Maris, C.D. Roberts, Int. J. Mod. Phys. **E12**, 297 (2003).
7. C.S. Fischer R. Alkofer, Phys. Rev. **D67**, 094020 (2003).
8. N.E. Mavromatos, J. Papavassiliou, , cond-mat/0311421, Invited review to appear in 'Recent Research Developments in Physics' (TRN) , and references therein
9. J.C.R. Bloch, *Few Body Syst.* **33**, 111 (2003).
10. F.D.R. Bonnet, P.O. Bowman, D.B. Leinweber, A.G. Williams, J.M. Zanotti, Phys. Rev. **D64**, 034501 (2001).
11. J.C.R. Bloch, A. Cucchieri, K. Langfeld, T. Mendes, hep-lat/0209040.
12. C. S. Fischer, F. Llanes-Estrada, R. Alkofer, hep-ph/0407294, Summary of a talk given at the international conference QCD DOWN UNDER 2004, Adelaide.
13. V.Šauli, *JHEP* 0302, 001 (2003).
14. V.Šauli, *J. Phys.* **G30**, 739 (2004).
15. Y. Nambu, Phys. Rev. **100**, 394 (1955).
16. Y. Nambu, Phys. Rev. **101**, 459 (1956).
17. C. De Witt, R. Omnes (editors), *Dispersion relations and elementary particles*, Hermann, Paris and John Wiley & Sons Inc. New York (1960).
18. S. Mandelstam, Phys. Rev. **115**, 1741 (1959).
19. R.J. Eden, P.V. Landshoff, D.I. Olive, J.C. Polkinghorn, *The Analytic S-matrix*, Cambridge (1966).
20. H. Umezawa, S. Kamefuchi, Prog. Theor. Phys. **6**, 543 (1951).
21. G. Källen, Helv. Phys. Acta. **25**, 417 (1952).
22. G.Kallen, Quantenelektrodynamik,in "Handbuch der Physik," Vol.5, Part I. J.Springer Verlag,Berlin ,1958; also Kgl. Danske Videnskab. Selskab, Mat. fys. Medd. **27**, No.12 (1953);
23. H. Lehmann, Nuovo Cim. **11**, 342 (1954).
24. S.Bauberger, F.A.Berends, M. Bohm, M.Buza, Nucl. Phys. **B434**, 383 (1995).
25. A. Bashir, R. Delbourgo, M.L. Roberts, J. Math. Phys. **42**, 5553 (2001).
26. S. Weinberg, Phys.Rev. **D8**, 3497 (1973).
27. N. Nakanishi, Graph Theory and Feynman Integrals, (eds. Gordon and Breach, New York,1971).
28. S. Deser, W. Gilbert, E.C.G. Sudarshan, *Phys. Rev.* **115**, 731 (1959).
29. M. Ida, Prog. Theor. Phys. **23**, 1151 (1960).
30. K. Kusaka, K. Simpson, A.G. Williams, Phys. Rev. **D 56**, 5071 (1997).
31. V.Šauli, J. Adam, Phys. Rev., **D67**, 085007 (2003).
32. D. Feldman, Phys. Rev. **117**,279 (1960).
33. C. Itzykson, J.B. Zuber, *Quantum Field Theory*, McGraw-Hill Inc. (1980).
34. R.J. Rivers, *Path integral methods in quantum field theory*, Cambridge University Press, 1987.

35. V.Šauli, *PHD Thesis*, hep-ph/0108160.
36. H. Bethe, E. Salpeter, *Phys. Rev.* **84**,1232 (1951).
37. G.C. Wick, *Phys. Rev.* **96**, 1124 (1954).
38. T. Nieuwenhuis, J.A. Tjon, *Few Body Syst.* **21**,167 (1996).
39. S. Ahlig, R. Alkofer, *Ann. Phys.* **275**, 113 (1999).
40. K. Kusaka, A.G. Williams, *Phys. Rev. D* **51**, 7026 (1995).
41. C. Savkli, F. Gross, J. Tjon, *Phys. Atom. Nucl.* **68**, 842 (2005); *Yad.Fiz.* **68**, 874 (2005).
42. S. Mandelstam, *Proc. Roy. Soc. A* **233**, 248 (1955).
43. F.T.Hawes, T.Sizer, A.G.Williams, *Phys. Rev. D* **51**, 3081 (1995).
44. F.T.Hawes, T.Sizer, A.G.Williams, *Phys. Rev. D* **55**, 3866 (1997).
45. K. Kondo, H. Nakatani, *Prog. Theor. Phys.* **88**, 737 (1992).
46. H. Pagels, *Phys. Rev.* **D21** ,2336 (1980).
47. S. Weinberg, *Phys. Rev.* **D19**, 1277 (1979).
48. B. Holdom, *Phys. Lett.*, **B150**, 301 (1985).
49. R.S. Chivukula, hep-ph/0011264
50. T. Appelquist, R. Shrock, *Phys. Rev. Lett.* **90**, 201801 (2003).
51. Neil D. Christensen, Robert Shrock, hep-ph/0501294.
52. R.Fukuda, T.Kugo, *Nucl. Phys. B* **117**, 250 (1976).
53. M.Gockeler, R. Horsely, V. Linke, P. Rakow, G.Schierholz, H. Stuben, *Phys. Rev. Lett.* **80**, 4119(1998).
54. L.D. Fadeev, V.N. Popov, *Phys. Lett.* **B25**, 29 (1967).
55. D. Binosi, J. Papavassiliou, *Phys. Rev. D* **65**, 085003 (2002).
56. D. Binosi, J. Papavassiliou, *J. Phys.* **G30**, 203 (2004).
57. N. K. Nielsen, *Nucl.Phys.* **B101** 173 (1975).
58. L.D. Landau, I.M. Khalatnikov , *Zh. Eksp. Teor. Fiz* **29** 89 (1956).
59. L.D. Landau, I.M. Khalatnikov , *Sov. Phys. JETP* **69** (1959).
60. M.Namiki, K.Okano, *Prog. Theor. Phys. Suppl.***111** , (1993).
61. 111 John M. Cornwall, *Phys. Rev. D* **26**, 1453 (1982).
62. 112 J.M. Cornwall, J. Papavassiliou, *Phys. Rev. D* **40**, 3474 (1989).
63. D. Zwanziger, *Phys. Rev.* **D69**,016002 (2004).
64. A. Salam, R. Delbourgo, *Phys. Rev.* **135**, 1398 (1964).
65. R.Delbourgo, R.B.Zhang, *J. Phys.* **17A**, 3593 (1984).
66. R. Delbourgo, *Austral. J. Phys.* **52**, 681 (1999).
67. J.S. Ball, T-W. Chiu, *Phys. Rev. D* **22**, 2542 (1980).
68. A. Bashir, A. Raya, *Phys. Rev.* **D66** 105005 (2002).
69. Alfredo Raya Montano, PhD Thesis, hep-th/0404138.
70. A. Bashir, M.R. Pennington, A. Raya, hep-ph/0511291
71. A. Bashir and A. Raya, *Nucl.Phys.* **B709** 307 (2005).
72. A. Arrizabalaga, J. Smit, *Phys.Rev.* **D66**,065014 (2002).
73. V. Miransky, *Nuovo Cim.* **A90**, 149 (1985).
74. V. Miransky, *Sov. Phys. ,JETP* **61**, 905 (1985).
75. J. Adam, P. Bicudo, V. Šauli, prepared for publication.
76. R. Alkofer, W. Detmold, C.S. Fischer, P.Maris, *Phys. Rev.*, **D70**, 014014 (2004).

77. M.B. Halpern, Prog. Theor. Phys. Suppl. **111**, 163 (1993).
78. A. Kizilersu, M. Reenders, M.R. Pennington, Phys. Rev. D**52**, 1242 (1995).
79. D.C. Curtis, M.R. Pennington, *Phys. Rev* **D42**,4165 (1990).
80. A. Bashir, M.R. Pennington, Phys. Rev. **D53**, 4694 (1996).
81. C.J. Burden, C.D. Roberts, Phys. Rev **D44**,540 (1991).
82. A. Bashir, A. Kizilersu, M.R. Pennington, Phys. Rev. **D62**,085000 (2000).
83. A. Bashir, R. Delbourgo, J. Phys. **A37**,6587 (2004).
84. A. Bashir, M.R. Pennington, Phys. Rev. **D50**, 7679 (1994).
85. A. Bashir, A. Raya, Nucl.Phys. **B709**, 307 (2005).
86. J.-P. Blaizot, E. Iancu, A. Rebhan, Phys. Rev. Lett. **83**2906 (1999).
87. J.-P. Blaizot, E. Iancu, Phys. Rev. **D63** (2001), 065003.
88. J.-P. Blaizot, E. Iancu, A. Rebhan, Phys. Lett. **B470**, 181 (1999).
89. G. Aarts, D. Ahrensmeier, R. Baier, J. Berges, J. Serreau, Phys. Rev. **D66**, 045008 (2002).
90. F. Cooper, J. Dawson, B. Mihaila, Phys.Rev. **D67**,056003 (2003), and references therein.
91. G. Aarts, Jose M. Martinez Resco, Phys. Rev. **D68**, 085009 (2003).
92. E. Braaten, E. Petitgirard, Phys. Rev. **D65**, 085039 (2002).
93. E. Braaten, E. Petitgirard, Phys. Rev. **D65**,041701 (2002).
94. J.O. Andersen, M. Strickland, Phys.Rev. **D71**, 025011 (2005).
95. J. Berges, hep-ph/0409233.
96. J.C.R. Bloch, Ph.D. thesis - University of Durham (1995), hep-ph/0208074.
97. J.C.R. Bloch, M.R. Pennington, Mod. Phys. Lett. A **10**, 1225, (1995).
98. J.C. Collins, A.J.MacFarlane, Phys. Rev. D **10**, 1201 (1974).
99. L.D. Landau, *On the Quantum Field Theory, in Niels Bohr and the Development of Physics*, ed. W. Pauli Pergamon, London (1955).
100. H.van Hees, J. Knoll, Phys.Rev. **D65**,105005 (2002).
101. F. Cooper, B. Mihaila, J.F. Dawson, Phys.Rev. **D70**,105008 (2004).
102. P. Maris, Phys. Rev. D **52**, 6087 (1995).
103. P. Maris, Int. J. Mod. Phys. A **7**, 5369 (1992).
104. A. I. Alekseev, hep-ph/0503242.
105. D.J. Gross, F. Wilczek, Phys. Pev. Lett. **30**, 1343 (1973).
106. H.D. Politzer, Phys. Pev. Lett. **30**, 1346 (1973).
107. C.D. Roberts, S.M. Schmidt, Prog. Part. Nucl. Phys. **45S1**, 103 (2000).
108. P. Maris and P.C. Tandy, nucl-th/0511017, contribution to the proceedings of LC05, Cairns, Australia, July 2005.
109. A. Bender, W. Detmold, C.D. Roberts, A.W. Thomas, Phys. Rev. **C65**, 065203 (2002).
110. F.J. Llanes-Estrada, P. Bicudo, Phys. Rev., **D68**, 094014 (2003).
111. P. Bicudo, Phys. Rev. **D69**, 074003 (2004).
112. C.S. Fischer, R. Alkofer, hep-ph/0411347.
113. L.D. Fadeev, V.N. Popov, Phys. Lett **25B**, 29 (1967).
114. A. Salam, Phys. Rev. **130**, 1287 (1963).
115. J. Strathdee, Phys. Rev. **135**, 1428 (1964).
116. R. Delbourgo, P.C. West, *J. Phys.* **A 10**, 1049 (1977).
117. R. Delbourgo, P.C. West, Phys. Lett. **B 72**, 96 (1977).
118. R.Delbourgo, Nuovo Cim. **49**, 484 (1979).

119. Y. Hoshino, hep-th/0202020.
120. M. Lavelle, Phys. Rev. **D44** R26 (1991).
121. M.A. Shifman, A.I. Vainshtein, V.I. Zakharov, Nucl. Phys. *B147*, 385 (1979).
122. G. Parisi, R. Petronzio, Phys. Lett. **94B**, 51 (1980).
123. R. Gupta et al., Phys. Rev. **D36**, 2813 (1987).
124. P. Marenzoni, G. Martinelli, N. Stella, M. Testa, Phys. Lett. **B318**, 511 (1993)
125. C. Bernard, C. Parrinello, A. Soni, Phys. Rev. **D49**, 1585 (1994).
126. J.I. Skullerud et al. (UKQCD Collaboration), Nucl. Phys. Proc. Suppl. **73**. 626 (1999).
127. A. Cucchieri, Phys. Rev. **D 60**,034508 (1999).
128. R. Alkofer, L. von Smekal, *Phys.Rept.* , **353**, 281 (2001).
129. S. Mandelstam, *Phys. Rev.* bf D20, 3223 (1979).
130. N. Brown, M.R. Pennington ,*Phys.Rev.* **D39**, 2723 (1989).
131. K. Buttner, M.R. Pennington, *Phys.Rev.* **D52**, 5220 (1995).
132. L. von Smekal, R. Alkofer, A. Hauck, *Phys. Rev. Lett.* **79**, 3591 (1997).
133. D. Atkinson, J.C.R. Bloch, *Phys.Rev.* **D58**, 094036n (1998)
134. D. Atkinson, J.C.R. Bloch, *Mod. Phys. Lett.* **A13**, 1055 (1998).
135. F.T. Hawes, C.D. Roberts, A.G. Williams, *Phys. Rev.***D49**, 4683 (1994).
136. C. Lerche, L. Smekal, *Phys.Rev.* **D65** ,125006 (2002).
137. K. Kondo, *Phys.Lett.* **B551**,324 (2003).
138. A. C. Aguilar, A. A. Natale, *JHEP* 0408 (2004) 057.
139. R. Alkofer, C.S. Fischer, H. Reinhardt, L. Smekal, *Phys.Rev.***D68**, 045003 (2003).
140. K. Kondo, hep-th/0303251.
141. V.A. Nesterenko, *Int. J. Mod. Phys.* **A18**,5475 (2003).
142. A.V. Nesterenko, J. Papavassiliou, *Phys.Rev.* **D71**,016009 (2005).
143. K. Langfeld, H. Reinhardt, J. Gattnar, *Nucl.Phys.* **B621**131 (2002).
144. A. Cucchieri, T. Mendes, A. R. Taurines, *Phys.Rev.* **D71**, 051902 (2005).